Clinical Anatomy 31:466–487 (2018)

ORIGINAL COMMUNICATION

Embryology of the Craniocervical Junction and Posterior Cranial Fossa, Part I: Development of the Upper Vertebrae and Skull

MOHAMMADALI M. SHOJA,[1] REBECCA RAMDHAN,[2] CHAD J. JENSEN,[2] JOSHUA J. CHERN,[3] W. JERRY OAKES,[4] AND R. SHANE TUBBS[3]*

[1]*Neuroscience Research Center, Tabriz University of Medical Sciences, Tabriz, Iran*
[2]*Department of Anatomical Sciences, St. George's University School of Medicine, Grenada*
[3]*Seattle Science Foundation, Seattle, Washington*
[4]*Children's Hospital, Birmingham, Alabama*

Although the embryology of the posterior cranial fossa can have life altering effects on a patient, a comprehensive review on this topic is difficult to find in the peer-reviewed medical literature. Therefore, this review article, using standard search engines, seemed timely. The embryology of the posterior cranial fossa is complex and relies on a unique timing of various neurovascular and bony elements. Derailment of these developmental processes can lead to a wide range of malformations such as the Chiari malformations. Therefore, a good working knowledge of this embryology as outlined in this review of its bony architecture is important for those treating patients with involvement of this region of the cranium. Clin. Anat. 31:466–487, 2018.

Key words: anatomy; Chiari malformation; hindbrain; spine

INTRODUCTION

In early development, during embryogenesis, the notochord is primarily formed. This is the key initiator in stimulating neural tube development, sclerotogenesis, and paraxial mesoderm patterning (Fan and Tessier-Lavigne, 1994; Ebensperger et al., 1995; Dockter et al., 2000a; Christ et al., 2004). Vertebral development was explained by Sensenig (1957) as comprising three overlapping stages, which additionally incorporated bony elements in the occipital region that fuse early to form the basiocciput and exocciput. The first stage occurs around the fourth week of gestation and highlights the maturation of the notochord. Specifics of notochordal development during early embryonic life are detailed and not the focus of review. The general aspects and features of notochordal development are schematized in Figure 1. The second stage occurs around the fifth and sixth weeks of gestation. It highlights the intense proliferation and migration of sclerotomic cells toward the notochord, formation of mesenchymal perinotochordal sclerotomes, expansion and patterning of the neural crest, and spinal nerve formation. The third and final stage commences around the middle of the sixth week, when chondrification and ossification take place.

SCLEROTOGENESIS AND DEVELOPMENT OF VERTEBRAE

Toward the end of the fourth week of gestation, the notochord induces ventromedial migration of mesenchymal cells from the condensed paraxial mesoderm of the somites, which encircle the notochord to become the primary sclerotomes. These primary sclerotomes are grossly segmented and this pattern of segmentation follows that in the respective somites. With the re-arrangement (or re-segmentation) of the primary sclerotomes, sclerotomal cells from differing somital origins pool together to form secondary

*Correspondence to: R. Shane Tubbs. E-mail: shanet@seattlesciencefoundation.org

Received 1 January 2018; Accepted 15 January 2018

Published online 9 March 2018 in Wiley Online Library (wileyonlinelibrary.com). DOI: 10.1002/ca.23049

TABLE 1. Some Developmental Anomalies and Osseous Variations of the Occipital Bone Including Manifestations of Occipital Vertebrae.

Anomaly or variation	Description	Reference(s)
Canalis basilaris medianus	Postnatal remnant of the cephalic notochord; presents as a well-corticated longitudinal canal in the midline of the basiocciput	Madeline and Elster (1995b)
Median basioccipital raphe	Midline trace of the median fusion of the parachordal plates	Madeline and Elster (1995b)
Longitudinal basioccipital cleft	Partial midline cleft in the basiocciput; is reminiscent of midline fusion of the bilateral parachordal plates	Madeline and Elster (1995b)
Cruciform sphenooccipital synchondrosis	Longitudinal anterior basioccipital and postsphenoidal clefts in conjunction with unossified sphenooccipital synchondrosis	Madeline and Elster (1995b)
Transverse (coronal) basioccipital cleft	Results from retention of the segmented nature of the basioccipital primordium; can traverse the basiocciput partially or completely; can be an incomplete groove or a complete gap; is radiographically similar to the sphenooccipital synchondrosis but is actually filled with fibrous tissue not cartilage; very rare	Kruyff (1967); Johnson and Israel (1979); Prescher (1997)
Basioccipital hypoplasia	A consequence of paraxial mesodermal insufficiency in the occipital region or premature closure of the sphenooccipital synchondrosis; associated with basilar invagination	Smoker (1994); Nishikawa et al. (1997); Noudel et al. (2009)
Fossa navicularis	A shallow depression measuring ~3 × 5 mm on the undersurface of the anterior portion of the basiocciput	Cankal et al. (2004)
Pharyngeal tubercle	A median tuberosity on the undersurface of the basiocciput about 1 cm anterior to the foramen magnum; is the point of attachment of the pharyngeal raphe; a tubercle of 1.5-2.0 cm diameter is radiographically apparent in 3.8% of cases	Robinson (1918); Hauser and De Stefano (1989); Finke (1964)
Bipartite hypoglossal canal	Division of the hypoglossal canal by a bony spicule; is a remnant of the hypochordal bow of S3	O'Rahilly and Müller (1984); Müller and O'Rahilly (2003)
Divided (bipartition of) occipital condyle	Partial or complete subdivision of the articular facet; can be unilateral or bilateral; associated with division of the superior articular facet of the atlas; has an incidence of ~5%	Tubbs et al. (2005); Kunicki and Ciszek (2005); Tillmann and Lorenz (1978)
Condylar hypoplasia	Underdevelopment of the occipital condyles; associated with a more horizontal than oblique orientation of the atlantooccipital joint and basilar invagination	Smoker (1994)
Occipitocondylar hyperplasia	Hypertrophy of the occipital condyles; can cause cervicomedullary compression	Ohaegbulam et al. (2005); Halanski et al. (2006)
Paracondylar (paramastoid or jugular) process	A pneumatized osseous process in the lateral condylar area (jugular process of the occipital bone) located between the occipital condyle and mastoid process at the point of insertion of the rectus capitis lateralis muscle; can be unilateral or bilateral; may or may not fuse with the transverse process of the atlas; has an incidence of 2–4%	Lang (2001); Tubbs et al. (2005); Anderson (1996); Taitz (2000); Prescher (1997)
Lateral (transverse) process of the occipital condyle	Is homologous to the transverse process of the atlas arising from the its lateral mass; is a proatlas remnant	Stratemeier and Jensen (1980); Gladstone and Erichsen-Powell (1915)
Prebasioccipital arch or anterior lip of the foramen magnum	A U-shaped ridge connecting the end of the occipital condyles; manifests as the ventral arch of the proatlas	Prescher (1997); Taitz (2000); Oetteking (1923)
Basilar process	Lateral tubercle and the remains of the prebasioccipital arch; a proatlas remnant; is sometimes considered a variant of or the same as the precondylar process	Prescher (1997); Oetteking (1923)
Condylus tertius	A downward bony projection located just at the anterior margin of the foramen magnum; associated with an increased prevalence of os odontoideum; has an incidence of ~1%	Smoker (1994); Prescher 1996, 1997)

TABLE 1. *Continued*

Anomaly or variation	Description	Reference(s)
Precondylar process or pseudocondylus tertius	A single median or two paramedian projection(s) from the inferior surface of the basiocciput located a few millimeters in front of the anterior margin of the foramen magnum; has an incidence of up to 25% in adults; is a proatlas remnant; is also regarded as an ossification in the median portion of the anterior atlantooccipital membrane; unlike the condylus tertius, it contains a sagittal canal	Vasudeva and Choudhry (1996); Prescher (1997); Hauser and De Stefano (1989)
Anteromedian tubercle of foramen magnum	A small median triangular tubercle projected horizontally backward from the anterior border of the foramen magnum; is distinct from the condylus tertius, which projects downward; can represent ossification of the attachment of the apical ligament	Lakhtakia et al. (1991); Prescher (1997); Oetteking (1923)
Posterior lip of the foramen magnum	A bony ridge extending from the posterior end of one or both occipital condyle(s) along the posterior foraminal margin; does not fuse posteriorly; can be hypertrophied and manifest as the bony excrescences around the posterior margin of the foramen magnum; remnants of the dorsal arch of the proatlas	Gladstone and Erichsen-Powell (1915); Prescher (1997); Menezes and Fenoy (2009); Oetteking (1923)
Kerckring or Kerckring-like ossicle(s)	A single median or paramedian ossicle at the lower edge of the supraocciput; there may be two paramedian ossicles, which then fuse to form a single median ossicle; appears in the fourth and fifth fetal months and usually fuses with the supraocciput before birth; rarely remains completely separated; although controversial, some have regarded it as a remnant of the proatlas	Piersol (1918); Le Double (1903); Caffey (1953); Madeline and Elster (1995b)
Accessory ossicle(s) of the innominate (posterior intraoccipital) synchondrosis	Is seen in 0.4% of newborns as 1–4 ossicles within the synchondrosis between the supraocciput and exocciput; can be large and protrude externally and internally; fuses with the supraocciput in the first year of life; the medially located ossicles can be considered as proatlas remnants	Caffey (1953)
Persistent transverse occipital fissure/suture	A fissure/suture between the intermediate and interparietal parts of the occipital squamous; is sometimes misnamed the mendosal suture	Lochmuller et al. (2011); Nayak et al. (2007); Tubbs et al. (2007)
Atlantooccipital assimilation	Partial or complete fusion of the atlas and occipital bone along the margin of the foramen magnum; associated with basilar invagination	Smoker (1994)

sclerotomes with a segmentation pattern, which follows that in the final vertebrae (Sensenig, 1957). Somitogenesis and the formation and rearrangement of primary sclerotomes all occur in a craniocaudal direction. Therefore, vertebral differentiation in the occipital and cervical regions precedes the development in the caudal region (Sensenig, 1957). Along with sclerotomal rearrangement, a subpopulation of sclerotomes, which were derived from its densely packed cellular region, migrate dorsolaterally around the neural tube and between the spinal nerves and ganglia to establish the mesenchymal primordia of the vertebral arch (Sensenig, 1957). The eventual chondrification of the mesenchymal primordium of each vertebra gives rise to the basic structure of the early vertebra, which comprises a cartilaginous centrum (the future vertebral body) and a neural arch around the neural tube (Robinson, 1918; Sensenig, 1957). It is crucial that the primary sclerotomes above and below the C2 vertebra adopt different rearrangement patterns in order to meet the anatomical and functional requirements of the craniovertebral junction above and the rest of vertebral column below.

THE DEVELOPMENT OF VERTEBRAE BELOW C2

The fundamental concepts in vertebral development below the axis (C2 vertebra) were recognized over a century ago (cf. Robinson, 1918) and concluded in the seminal work of Sensenig (1957). By the end of the first month of embryonic development, the notochord and neural tube are bounded by the skeletogenic mesodermal tissue composed of primary sclerotomes, which were derived from the ventromedial parts of somites that were found on either side of the neural tube. Dockter et al. (2000b) explained that the

cell distribution in each primary sclerotome is heterogeneous, with craniocaudal and mediolateral gradients. There is a greater cellular density in the caudal and lateral portions of the sclerotomes than the cranial and medial portions. The initial segmentation of primary sclerotomes follows the somital pattern; however, re-segmentation occurs soon after. The fissure of von Ebner separates the two halves of the primary sclerotomes on the lateral region where the spinal nerves and blood vessels emerge. The loosely cellular cranial half of each primary sclerotome combines with the densely cellular caudal half of the sclerotome above to become the secondary sclerotome corresponding to the future vertebra (Fig. 2). After dorsolateral migration of some of the sclerotomal cells, a dense lateral mass and a central mass (containing dense upper and loose lower regions) are apparent in each secondary sclerotome (Fig. 2). The dense lateral mass gives rise to the vertebral arch, which includes the pedicle, articular facets and lamina, and the larger lower loose region within the central mass gives rise to the centrum (body) of the vertebra. The narrow band of densely cellular sclerotomal tissue retained between the centra of the secondary sclerotomes is sometimes referred to as the hypochordal bow (Robinson, 1918; O'Rahilly and Müller, 1984), perichordal disc (Sensenig, 1957), hypocentrum (Ganguly and Roy, 1964), or intercentrum (Bailey et al., 1983). In this review, the term "hypochordal bow" is preferred. It is believed that the hypochordal bow degenerates into the fibrous part of the intervertebral disc (Robinson, 1918).

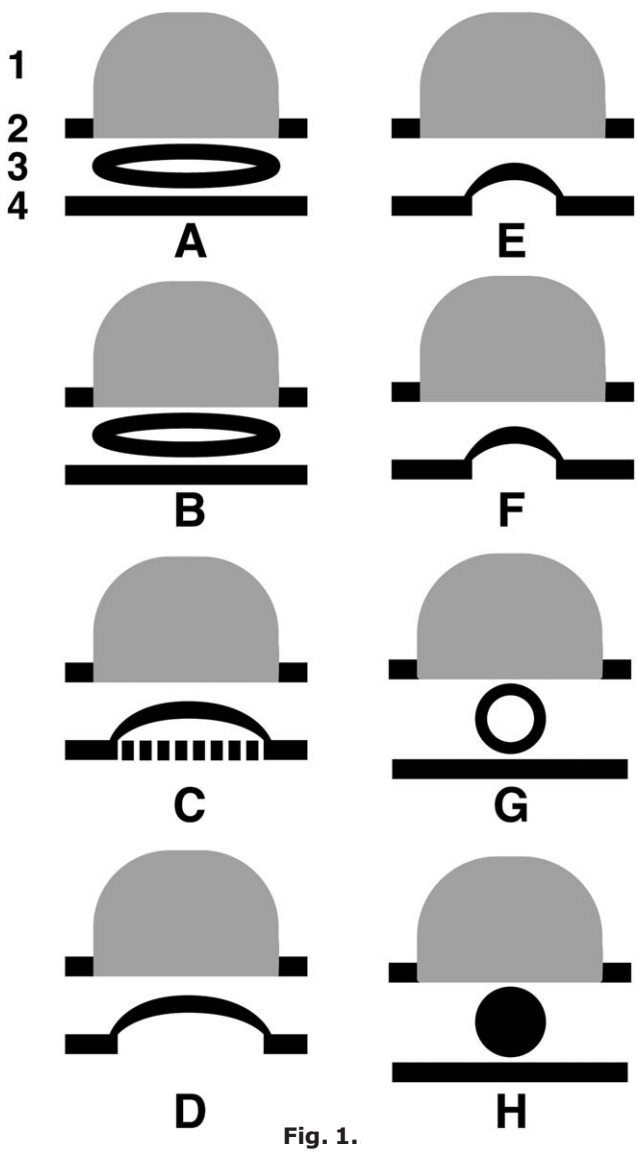

Fig. 1.

DEVELOPMENT OF THE CRANIOCERVICAL JUNCTION

Ludwig (1957), O'Rahilly and Müller (1984), and Müller and O'Rahilly (1994, 2003) have contributed extensively to current knowledge of craniovertebral junction development. The superior four somites are occipital somites 1–4. The ventromedial migration of sclerotomal cells from somites 1–4 toward the cephalic notochord gives rise to primary occipital sclerotomes 1–4 (O1–4). The hypoglossal nerve rootlets course laterally between the hypochordal bows of the occipital sclerotomes and the C1 spinal nerve between the hypochordal bows of O4 and sclerotome 5 (S5 or first cervical sclerotome). Initially, occipital sclerotomes 1–3 join to form the main portion of the mesenchymal basiocciput (O'Rahilly and Müller, 1984). In an embryo of 9 mm crown-rump length (CRL: approximately the fifth week of gestation), the hypochordal bows of O4 (proatlas) and S5 (atlas) are distinct in the craniovertebral junction (Ludwing, 1957). The notochord travels dorsal to the hypochordal bows (Ludwing, 1957). The rostral O1-O3 hybrid and O4

Fig. 1. Schematized drawing of a transverse section through the midportion of the embryonic plate showing notochordal development and maturation. Upon formation of the primitive streak from the ectoderm on the dorsal midline of the embryonic plate, the mesodermal precursor cells originating from the primitive streak migrate between the ectoderm and endoderm (not shown here). The longitudinal midline condensation of the mesodermal cells forms the head process or notochordal plate in front of the primitive streak. **A**, The notochordal plate (3) has a lumen, a floor next to the endoderm (4), and a roof next to the neural plate (1) of the ectoderm (2). **B**, The floor of the notochordal plate fuses with the endoderm. **C** and **D**, The floor then disappears, leaving the roof of the notochordal plate (known as the notochordal groove at this stage) attached to endoderm on either side. **E** and **F**, The notochordal groove deepens and its margins approximate each other by the growth of the endoderm. **G**, Following the fusion of the margin of the notochordal groove, the notochordal tube is formed and is liberated from the endoderm. **H**, The lumen of the notochordal tube disappears and the tube solidifies to form the mature notochord. This description is based on Frazer (1931).

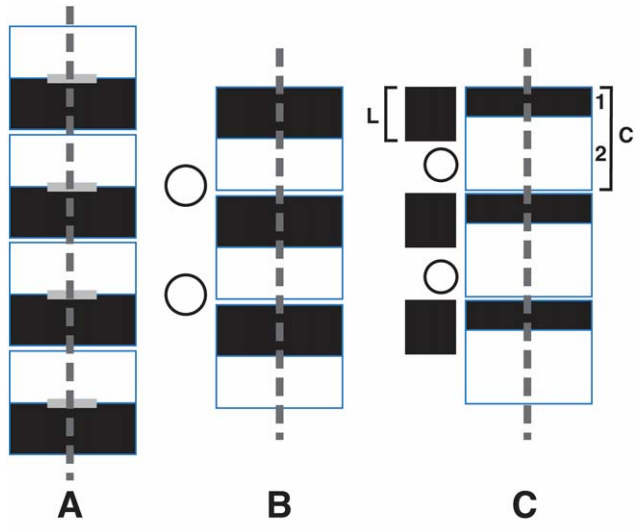

Fig. 2. Simplified model of the re-arrangement of primary sclerotomes and development of vertebrae below C2. **A** shows primary sclerotomes with loose upper (white) and dense lower (dark) regions partially separated by the fissures of von Ebner (grey horizontal bars). The longitudinal dashed line represents the notochord. **B** shows the secondary sclerotomes following re-arrangement. The circles represent the spinal root ganglia, nerves and blood vessels emerging at the level of the loosely cellular region. **C** shows the sclerotomic primordia of the vertebrae following dorsolateral migration of a subpopulation of cells from the dense region between the spinal root ganglia and nerves. At this stage, the central (C) and lateral (L) masses are discernible. The central mass is composed of the hypochordal bow (1) and centrum (2). [Color figure can be viewed at wileyonlinelibrary.com]

join together in an embryo of 9–11 mm CRL (approximately the sixth week of gestation) to form a mesenchymal O1–04 hybrid surrounding the cephalic end of the notochord (O'Rahilly and Müller, 1984). This mesenchymal hybrid is termed chordal cartilage after chondrification occurs later in gestation. The hypochordal bow of O2 is small, disappears medially and fuses with the hypochordal bow of O3 laterally. The dorsolateral extensions of the hypochordal bows of O2-O4 create the lateral masses. Further dorsal extension of these masses adds to the development of the exocciput, homologous to the neural arch of a typical vertebra. The portion of the exocciput rostral to the hypoglossal nerve and canal is formed from O3 and the caudal portion is formed from O4. Ultimately, the lateral masses of S3 and S4 fuse to create a single exocciput ventral and dorsal to the hypoglossal canal. Loosely packed sclerotomal cells between the hypochordal bows of the proatlas and atlas, corresponding to the centrum of primary sclerotome 5, contribute to the occipital condyles laterally and the tip of the odontoid process of the axis medially (O'Rahilly and Müller, 1984; Müller and O'Rahilly, 1994).

A simplified model of craniovertebral junction development is presented in Figure 3. The hypochordal bow of O3 degenerates except for its lateral projections, which are exaggerated by fusing with the hypochordal bow of O2 and contribute to the exocciput. At 5 weeks of gestation, the hypochordal bow of O3 is noticed laterally above and anterior to the hypochordal bow of O4 (O'Rahilly and Müller, 1984). An osseous separation within the hypoglossal canal is formed by the medial remnant of the hypochordal bow of O3 (Müller and O'Rahilly, 2003), and the median part of the hypochordal bow of O4 remains as a continuous mass across the midline that begins fusing with the remainder of the basiocciput rostrally during the mesenchymal stage (O'Rahilly and Müller, 1984). After chondrification its fusion is completed, forming the basion. The hypochordal bow of S5 forms the anterior arch of the atlas and disappears from between the loosely packed regions of the S5 and S6 sclerotomes (Müller and O'Rahilly, 2003). The lateral mass of S5 (C1) encompasses the odontoid process and forms the neural/posterior arch of the atlas (Müller and O'Rahilly, 1994, 2003), whereas the lateral mass of S6 forms its neural arch.

DEVELOPMENT OF THE OCCIPITAL CONDYLE

The occipital condyles are two semilunar prominences with an inward concavity and outward convexity, which appear on the anterolateral region of the foramen magnum (Ganguly and Roy, 1964). The condyles comprise a cartilaginous articular facet that is convex ventrodorsally and mediolaterally, and an osseous portion. The medial region of the condyle tends to be larger than the lateral region. During embryogenesis, the sclerotomic primordia of the occipital condyles are derived from the hypochordal bow of S4 and the loosely packed region of S5. After chondrification in the occipital region, the basioccipital and exoccipital components are united and the ossification centers appear independently within these segments. The ventral and dorsal regions of the exoccipital and suboccipital ossification centers grow and meet each other but remain separated by a synchondrosis (known as the anterior intraoccipital synchondrosis), which traverses the occipital condyle. As a result, the occipital condyle is divided by a cleft corresponding to the unossified anterior intraoccipital synchondrosis and this is seen in children (Tillmann and Lorenz, 1978). It should be noted that the region of condyle anterior to the synchondrosis is the basioccipital area, which is smaller than the region posterior to the synchondrosis, the exoccipital area (Tillmann and Lorenz, 1978). The anterior intraoccipital synchondrosis ossifies in a mediolateral direction (Tillmann and Lorenz, 1978), a process that begins around 1–2 years of age and is completed by 7–10 years of age (Madeline and Elster, 1995a). From then onwards, the occipital condyle presents as a single osseous prominence with a uniform articular facet. Sometimes, adults have a transverse division of the articular facet, which can result from maceration of its midportion (Tillmann and Lorenz, 1978).

A bony ridge (prebasioccipital arch) sometimes connects the anterior ends of the occipital condyles in

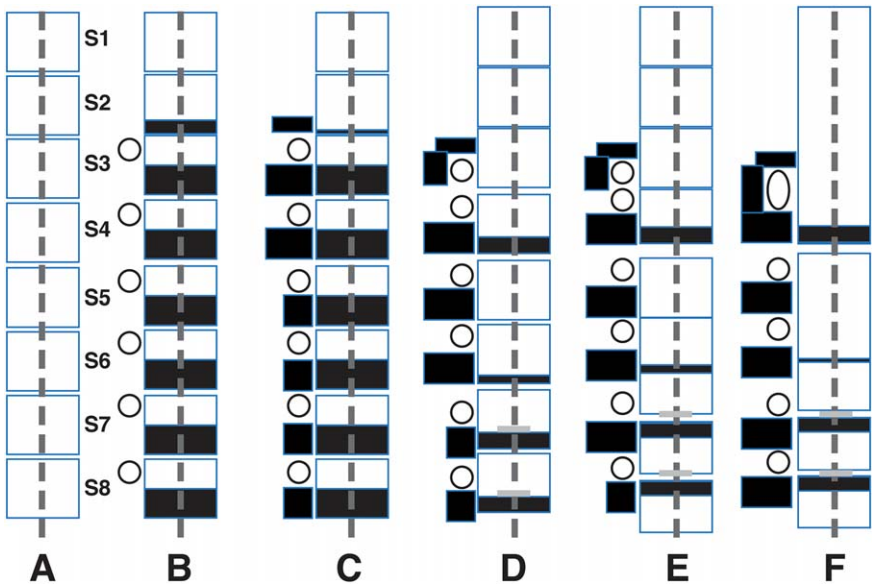

Fig. 3. A simplified model of craniovertebral junction and upper cervical vertebral development based on O'Rahilly and Müller (1984), Müller and O'Rahilly (1994) and Sensenig (1957). **A**, With migration of ventromedial somital cells toward the notochord, segmented sclerotomes are formed. The longitudinal dashed lines represent the notochord. **B**, The lower half of occipital sclerotomes 2, 3 and 4 and cervical sclerotomes undergo condensation (dark regions). Segmental ganglia and nerves, represented by circles, develop from the neural crest. **C,** The cells from the caudal half of the sclerotome migrate dorsolaterally through the interganglionic space. Note the craniocaudal gradient in the development of the neural arches, with more dorsolateral extension of the hypochordal bows in the occipital region than in the cervical region. At this stage, the median (central) and lateral segments are established, roughly representing the centrum and neural arch of a developing vertebra. The median part of the hypochordal bow of S2 begins to disappear. The median segments of S3-S8 are still composed of dense caudal and loose rostral parts. **D,** The dense caudal parts of the centra of S2 (or O2) and S5 (C1) disappear. The dense caudal parts of the other sclerotomes are now smaller. The fissures of von Ebner (horizontal grey bars) separate the caudal and loose rostral parts of S7 and S8 (C3 and C4, respectively). The median portion of the hypochordal bow of S3 disappears. The lateral mass derived from the hypochordal bow of S2 is fused with the hypochordal bow of S3 laterally, leaving the two hypoglossal nerve rootlets within in a single canal. **E,** The re-arrangement at the S7–9 centra occurs in such a way that the dense caudal part of S7 joins the loose rostral part of S8 (S7–8 fusion or future C3 vertebra) and the dense caudal part of S8 joins the loose upper part of S9 (S8-S9 fusion or future C4 vertebra). S9 is not shown in a-d. The centra of S1 to S4 fuse to form the basiocciput. The centra of S5 and S6 and the loose rostral part of the S7 centrum fuse to form the dens and body of the C2 vertebra. Note the hypochordal bows of S3 and S4 are fused laterally. **F,** The final re-arrangement of the occipitocervical junction is achieved. Note the hypoglossal nerve within the exocciput formed by fusion of the lateral bars (or extensions) of the hypochordal bows of O2-O4. The lateral bars of S7 and S8 form the neural arches of C3 and C4. Fusion of the upper dense parts of S7–8 forms intervertebral disc C2-C3 and fusion of the upper dense parts of S8-S9 forms intervertebral disc C3-C4. The development of the remaining vertebrae is similar to that of the C3 and C4 vertebrae. [Color figure can be viewed at wileyonlinelibrary.com]

front of the anterior rim of the foramen magnum (Oetteking, 1923; Prescher et al., 1996; Prescher, 1997; Taitz, 2000; Pang and Thompson, 2011). If the medial part of this ridge disappears, its lateral part will be retained unilaterally or bilaterally, in which event it would either remain ridge-like or appear bumpy and be termed the basilar process (Prescher et al., 1996). On the other hand, if the lateral part were to disappear, the medial part of the ridge could remain as a single median or two paramedian projections (Prescher et al., 1996; Vasudeva and Choudhry, 1996). These variants include the pseudocondylus tertius (Prescher et al., 1996; Prescher, 1997) or precondylar process (Vasudeva and Choudhry, 1996), and the true condylus tertius (Prescher, 1997; Pang and Thompson, 2011) (Fig. 4). The true condylus tertius is found just at the anterior rim of the foramen magnum. The precondylar process, which is a continuation of the anterior end of the occipital condyle (Prescher et al., 1996), is positioned slightly anterior to the foramen magnum. Both the precondylar process and the condylus tertius are derivatives of the hypochordal bow of the proatlas (Prescher et al., 1996). These bony outgrowths at the anterior margin of the foramen magnum are thus remnants of the anterior arch of the proatlas.

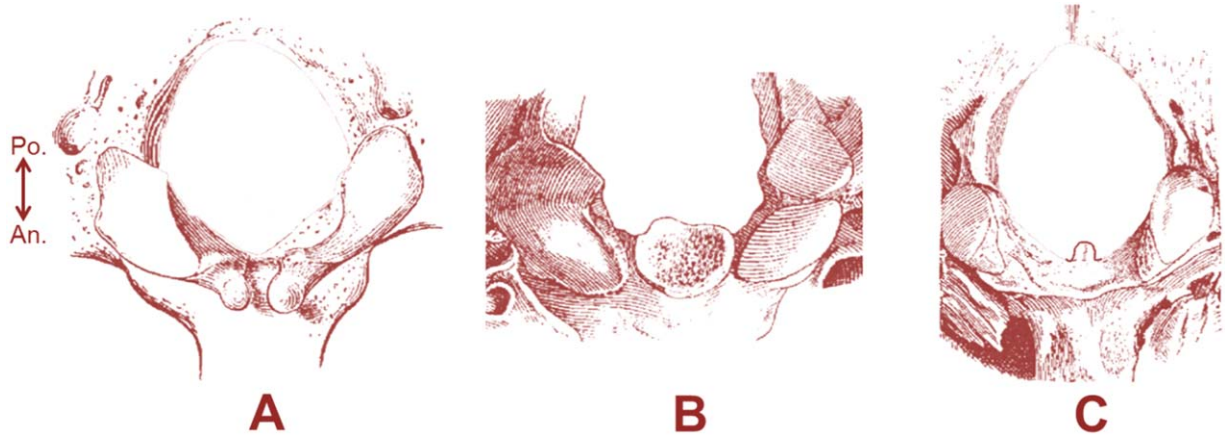

Fig. 4. The remnants of the anterior arch of the proatlas (reproduced from Oetteking (1923) with permission from John Wiley and Sons). The arrow shows the orientation of the specimens: An., anterior; Po., Posterior. **A** shows two basilar processes. Some regard these as the paremedian precondylar processes. **B** shows a single large condylus tertius. **C** shows a backward spur-like projection from the median portion of the anterior margin of the foramen magnum. Some advocate that this spur-like projection is not derived from the proatlas but represents ossification of the attachment of the apical ligament (Oetteking, 1923; Tubbs et al., 2000). [Color figure can be viewed at wileyonlinelibrary.com]

PROATLAS SEGMENTATION MALFORMATION AND VARIABLE MANIFESTATIONS OF THE PROATLAS

The proatlas, which can be found in some lower vertebrates, is a separate and unique atlas-like vertebra partitioned between the occipital bone and the atlas (Rao, 2002; Scheuer and Black, 2004). In contrast to a typical developing vertebra, the hypochordal bow of S4 never fuses with the centrum of S5 under normal conditions in man. Instead, it partially regresses and normally only contributes to the inferior portion of the basiocciput and the caudal part of the exocciput. The apex of the dens and the medial portion of the apical ligament are formed from the centrum of S5, which also contributes to formation of the lateral regions of the occipital condyles. This unique craniovertebral sclerotomal segmentation pattern dictates that the mesodermal constituents of the proatlas in man should be integrated into the occipital bone and axis. An array of osseous anomalies and variations can arise from the craniovertebral junction if: (a) this pattern of segmentation in the craniocervical junction is disordered; (b) the mesodermal constituents of the proatlas are distributed abnormally; (c) the hypochordal bow of S4 hypertrophies or fails to regress partially; or (d) the centrum of S5 abnormally tends to be liberated from the axis or fuses with the hypochordal bow of S4. The term "proatlas segmentation failure or malformation" has been applied to this ontogenetic error by several authors (Menezes and Fenoy, 2009; Goel and Shah, 2010; Xu et al., 2010). The associated anomalies or variations are collectively referred to as "proatlas remnants" or "manifestations of the proatlas," which are grouped under a broader category of "manifestations of the occipital vertebrae" (Table 1) (Csakany, 1957; Denisov and Kabak, 1984; Menezes, 1995; Prescher, 1997; Goel and Shah, 2010; Xu et al., 2010). In an evolutionary sense, the proatlas segmentation malformation represents a phylogenetic regression in the ontogeny of the craniovertebral junction with an attempt to retain the proatlas and liberate it from the occipital region (Gladstone and Erichsen-Powell, 1915; Stratemeier and Jensen, 1980). To our knowledge, there has only been only one reported case of a persistent proatlas as an additional atlas-like vertebra in the human species (Tsuang et al., 2011; Shoja et al., 2012a,b).

With such a complicated process, it is not surprising that anatomical presentations of the proatlas segmentation malformation are quite variable, some being more clinically significant than others. Some of the less clinically significant remnants of the proatlas, such as the basilar and precondylar processes and prebasioccipital arch, were discussed earlier. The clinically significant anomalies have an incidence rate of approximately 1.4%. They often result in compression of the lower brain stem (Menezes and Fenoy, 2009) and sometimes manifest as anomalous bony excrescences around the foramen magnum (Stratemeier and Jensen, 1980; Menezes and Fenoy, 2009). Normally, the tip of the odontoid process is not present and the basiocciput tends to be elongated and to protrude posteroinferiorly into the foramen magnum (Menezes, 1995; Menezes and Fenoy, 2009). This basioccipital protrusion is embryologically derived from the centrum of S5. Occasionally, the apex of the dens is present but is small and malformed. If there is no hypoplasia of the odontoid, the posteroinferiorly directed median bony projection at the anterior margin of the foramen magnum is the third occipital condyle (condylus tertius), which sometimes articulates with the apex of the dens or the anterior arch of the atlas (Prescher, 1997). As the notochord travels toward the back of the hypochordal bow of S4, the

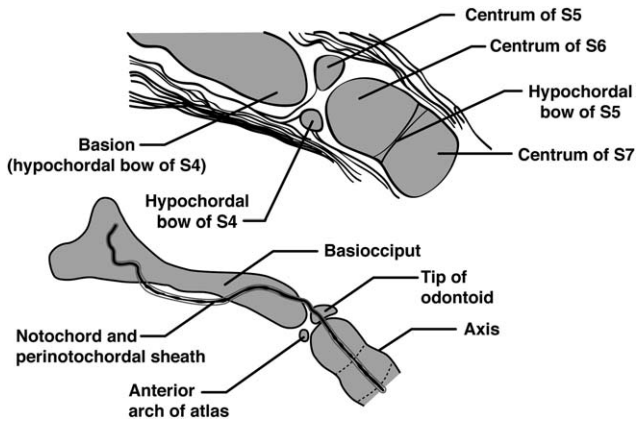

Fig. 5. Embryogenesis of the proatlas segmentation malformation - os terminale persistens (Bergman's ossicle) variant (after Gladstone and Erichsen-Powell, 1915). The upper and lower images show the mesenchymal/chondrified and osseous stages of the craniocervical junction, respectively. In the upper image, a small segment of notochord (star) is shown traversing between the centra of S5 and S6. In the lower image, the original fetal position of the notochord is superimposed on the components of the craniocervical junction. Note that the hypochordal bow of S4 contributes to the basion, and the centrum of S5 to the tip or apophysis of the odontoid. Normally, the centra of S5–7 fuse to form the dens and body of the axis. Failure of fusion leads to the formation of an independent center for chondrification and ossification in the S5 centrum and results in the tip of the odontoid being isolated, giving rise to os terminale persistens. On the other hand, if mesenchymal fusion and chondrification of the dens occur normally, the tip of the odontoid can be separated from the dens by an intervening synchondrosis derived from the vestigial remnant of the S5 hypochordal bow. This synchondrosis usually ossifies, and failure of its ossification also gives rise to os terminale persistens. The notochord has an S-shaped course through the basiocciput and passes through the os terminale persistens; it is located on the ventral surface of the basiocciput at its midportion and runs obliquely within its rostral and caudal parts (Gasser, 1976).

osseous anomalies in front of the apical ligament, such as the condylus tertius, represent the derivatives of the hypochordal bow. The apical ligament attaches to the basion over the condylus tertius (Ganguly and Roy, 1964). A triangular projection from the anterior margin of the foramen magnum, medial indentation from the occipital condyle and non-fusion, inward displacement and hypertrophy of the condyle, os terminale persistens (Fig. 5) and os odontoideum are among the clinically significant variants of proatlas remnants (Stratemeier and Jensen, 1980; Menezes and Fenoy, 2009; Pang and Thompson, 2011). Menezes (1995) found that only eight patients had clinically significant proatlas segmentation malformations out of 100 with Chiari malformation and craniovertebral junction anomalies. Likewise, hindbrain herniation accompanied proatlas segmentation malformations in 33% of cases (Menezes and Fenoy, 2009).

OSSIFICATION OF THE ATLAS

As stated earlier, the mesodermal primordium of the atlas is derived from the hypochordal bow of S5. Ganguly and Roy (1964) believed that before the embryo attains a CRL of 30 mm (approximately the eighth gestational week), the precartilaginous proatlas is divided and its dorsal caudal half incorporates into the cartilaginous primordium of the atlas while its ventral cranial part incorporates into the occipital cartilage at the anterior margin of the foramen magnum. This view is held by some recent authors (Menezes, 2008; Menezes and Fenoy, 2009) but its accuracy is uncertain. This is because the embryonic specimens presented by Ganguly and Roy (1964) lacked 11–30 mm CRL embryo stages, which encompass a period of substantial development in the craniovertebral junction. Macalister (1893) studied the developmental anatomy of the atlas thoroughly and reported that the ring of the atlas is completely chondrified at the fifth week of gestation. By the seventh week, two ossification centers appear at the root of the posterior arch close to the lateral masses, which grow in a retrograde direction to form the right and left posterior bony hemi-arches. This growth continues after birth until the right and left hemi-arches of the posterior arch fuses and closes in the dorsomedian plane at 4 years of age. The bilateral ossification centers also extend forward into the lateral masses and outward into the transverse processes (Macalister, 1893). There is a delay in the ossification of the anterior arch, which commences during the first year of life. Initially, two unequally sized ossification centers appear in the median part of the cartilaginous anterior arch, which rapidly fuse to form a single dominant ossification center; this grows backwards and laterally to join the lateral mass by the fifth year of age (Macalister, 1893). If there is failure in the development of the median ossification centers of the anterior arch, ossification will then proceed to the midline from the lateral masses of the atlas (Allen, 1879).

ATLANTOOCCIPITAL ASSIMILATION AND OTHER DEVELOPMENTAL ANOMALIES OF THE ATLAS

Occipitalization of the atlas, or atlantooccipital assimilation/fusion, is a process by which the atlas is either completely or partially fused with the occipital bone and is recognized as one of the most common anomalies of the craniovertebral junction (Chopra et al., 1988). Its prevalence ranges from 0.5% to 3% in different series (Bergman et al., 1996; Gholve et al., 2007; Kassim et al., 2010) and it appears to have a multifactorial causation, often aggregated in families (Kalla et al., 1989). The syndromic forms of atlantooccipital assimilation have been associated with Klippel-Feil syndrome and DiGeorge syndrome (Gholve et al., 2007; Menezes, 2008). Embryologically, the assimilation takes place when the primordia of the atlas and occiput are still cartilaginous (Macalister, 1893), but it is questionable whether this fusion can also occur in the early mesodermal stage. The

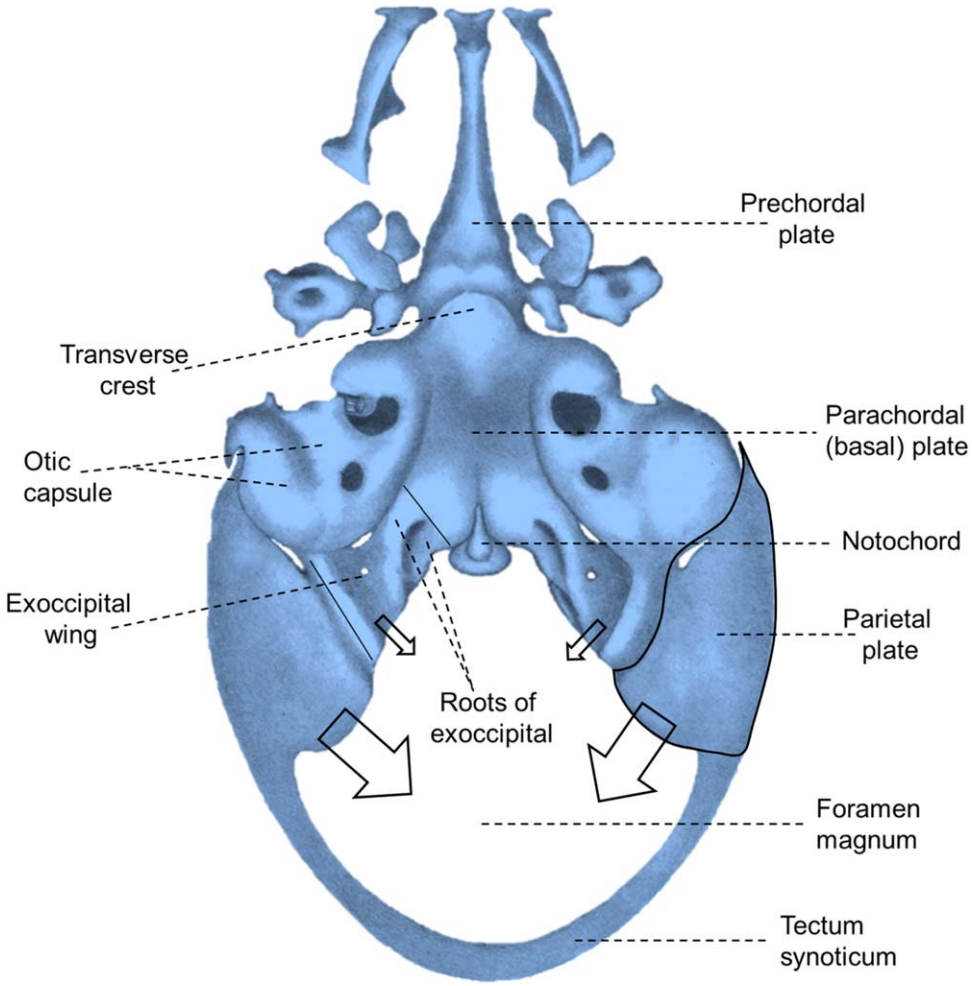

Fig. 6. Basichondrium of a 20 mm CRL embryo, ~8th week of fetal life (reproduced with some modifications from Kernan, 1916). The foramen magnum is very large at this stage. The exocciput is shown between two solid lines on the left side. The territory of the parietal plate is marked on the right side. The parietal plate of the occipital bone is anteroinferiorly fused with the otic capsule and posteroinferiorly with the exocciput, and extends posteriorly as the tectum synoticum. The caudal portion of the prechordal cartilage contributes to the basisphenoid, and the rest of it and the appendages develop into the anterior basicranium (Parsons, 1911). [Color figure can be viewed at wileyonlinelibrary.com]

anterior arch of the atlas fuses with the basion at the anterior margin of the foramen magnum, the posterior arch with the lower end of the supraocciput at the posterior margin of the foramen magnum, the superior articular facet with the occipital condyles anterolateral to the foramen magnum, and the transverse process of the atlas with the jugular process of the occipital bone (Allen, 1879; Macalister, 1893). Atlantooccipital assimilation results in a 15–35% reduction in the surface area of the foramen magnum (Tubbs et al., 2011) and is occasionally associated with os odontoideum and basilar invagination (Gholve et al., 2007). An animal model suggests that aberrations in homeobox (*Hox*) gene expression are associated with atlantooccipital assimilation (Condie and Capecchi, 1993). The family of highly conserved transcription regulatory proteins encoded by *Hox* genes is important in patterning and determining the segmental fate of the axial skeleton in vertebrates (Burke et al., 1995; Ferrier and Holland, 2001; Pourquié, 2009). In an evolutionary sense, and unlike the proatlas segmentation malformation, atlantooccipital assimilation represents phylogenetic progression in the ontogeny of the craniovertebral junction with an attempt to integrate an additional vertebra into the occipital region (Gladstone and Erichsen-Powell, 1915; Stratemeier and Jensen, 1980).

There have been reports of other developmental anomalies of the atlas (Allen, 1879; Macalister, 1893; Pang and Thompson, 2011). Defects (hypoplasia, dysplasia, agenesis, or clefts) in the anterior arch are less common than in the posterior arch. In a series of 21

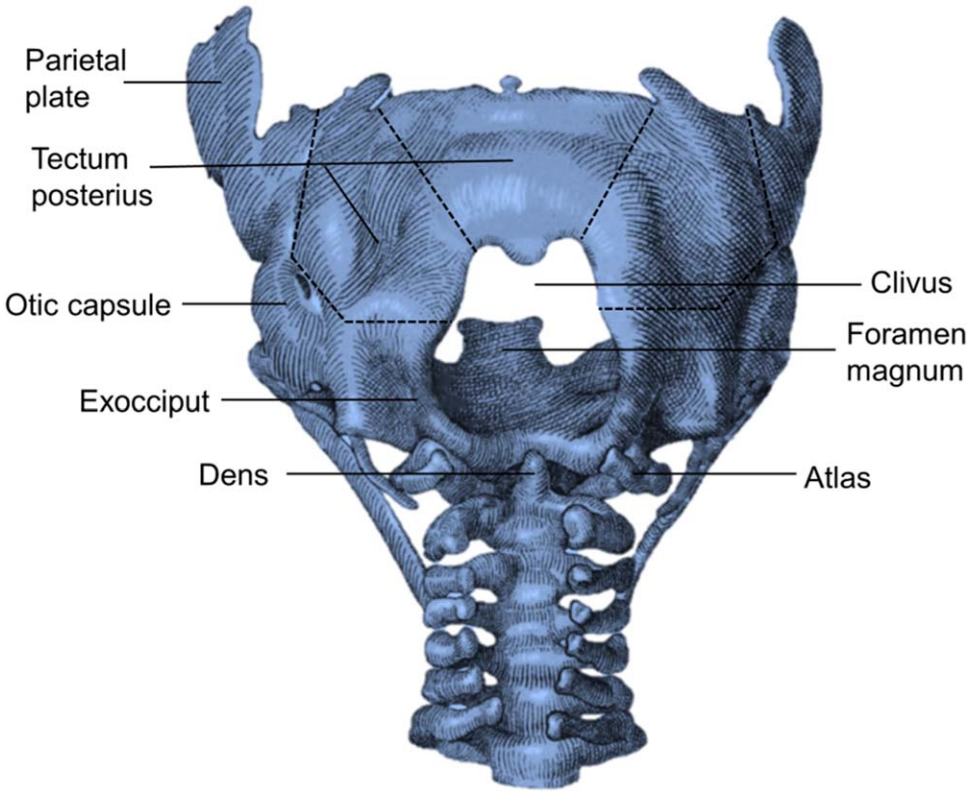

Fig. 7. The posteroinferior aspect of the basichondrocranium and occipital region of a 43 mm CRL fetus, ~12th week of fetal life (reproduced with modifications from Macklin, 1921). The tectum synoticum is regressed and the upper part of the posterior border of the parietal plates is free. The tectum posterius is derived from the parietal plates and exoccipital wings and is arbitrarily composed of two lateral pieces and a central piece (marked by dashed lines). At this stage, ossification progresses in the central part of the tectum posterius, the anterior (root) portion of the exocciput and the caudal portion of the basiocciput. [Color figure can be viewed at wileyonlinelibrary.com]

patients with either confirmed or suspected Chiari I malformation, agenesis of the anterior or posterior arches of the atlas or variable degrees of atlantooccipital assimilation were the most frequent osseous anomalies at the craniovertebral junction (Davies, 1967). In another series that involved 100 patients with Chiari malformation and concomitant craniovertebral junction anomalies, atlantooccipital assimilation was found in 92 (Menezes, 1995). These observations suggest that anomalies of the atlas are familiar in patients with hindbrain herniation and could indicate a common underlying ontogenetic error or could actually entail a cause-effect relationship.

BASICRANIAL DEVELOPMENT

The basicranium is composed of a flat anterior part and an oblique posterior part (clivus). The posterior part comprises basisphenoidal (anterosuperior) and basioccipital (posteroinferior) segments that are joined by an intervening sphenooccipital synchondrosis. The rostral end of the notochord delineates the caudal part of the sphenooccipital synchondrosis. The development of the basicranium proceeds in three stages: mesenchymal condensation, chondrification and ossification (Friede, 1981; Lemire, 2000). Once the mesenchymal (desmal or blastemal) basicranium is formed, chondrification and ossification take place in a posteroanterior direction with the posterior cranial fossa being the first and the anterior fossa the last to chondrify or ossify (Friede, 1981). Chondrification is completed during the third month of gestation. Chondrification and ossification are overlapping stages separated in space. In simpler terms, while chondrification is occurring in the anterior portion of the basicranium, the posterior basicranium begins ossifying (Friede, 1981). What follows relates to the posterior basicranium, which contributes to the formation of the posterior cranial fossa.

The segmented (sclerotomal) nature of the developing basiocciput was first discovered by Froriep in calves, Weiss in rats and Levi in humans (cf. Schäfer et al., 1908). The initial mesenchymal primordium of the basicranium was found to occur during the first month of gestation. Chondrification appears in the basioccipital region during the second month (Schäfer et al., 1908). Initially, two longitudinal cartilaginous plates (also referred to as parachordal plates) are

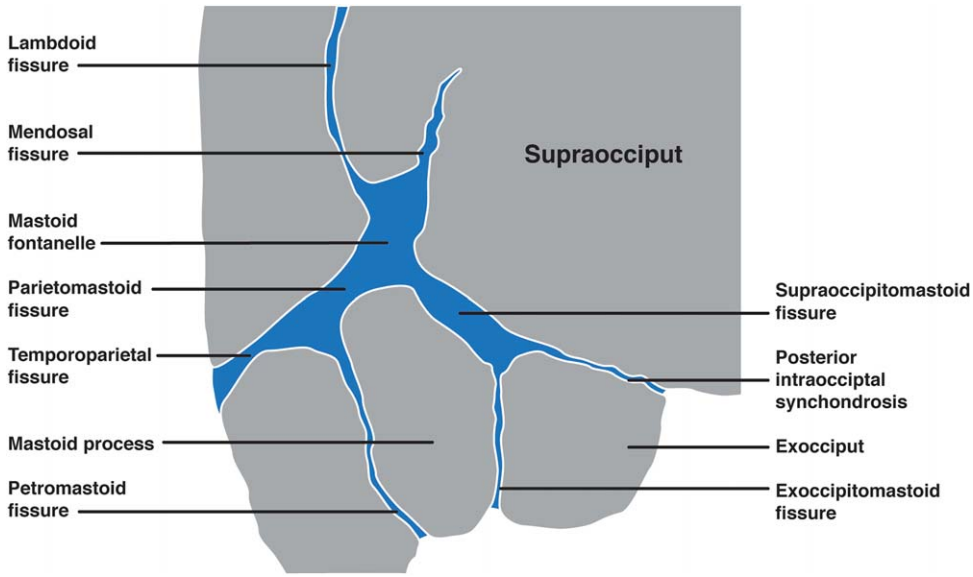

Fig. 8. Schema showing the mastoid fontanelle and its related cartilaginous fissures at birth. The fissures are replaced by the sutures in the adult skull, and some sutures are obliterated completely when the bones fuse. The mastoid fontanelle seems to be the remnant of the fetal parietal plate. The mendosal fissure is the remnant of the tectum synoticum (Niida et al., 1992). [Color figure can be viewed at wileyonlinelibrary.com]

formed on either side of the cephalic notochord around the fifth week of gestation (Schäfer et al., 1908; Gasser, 1976; Friede, 1981). Simultaneously, the cartilaginous otic capsule is also developing but is separate from the parachordal cartilage (Schäfer et al., 1908; Friede, 1981). The two parachordal plates fuse across the midline to form a single plate, known as the basal or chordal plate, surrounding the notochord (Schäfer et al., 1908; Friede, 1981). The cartilaginous otic capsule is then incorporated into the basal plates laterally (Schäfer et al., 1908). The segmented nature of the basiocciput begins to disappear during the late mesenchymal stage and is totally lost with fusion of the cartilaginous centers (Schäfer et al., 1908; Parsons, 1911). The basal cartilage is divided caudally and each division extends dorsolaterally in a horizontal plane and on either side of the foramen magnum as the exoccipital plate, that is, the cartilaginous primordium of the exocciput (Schäfer et al., 1908; Parsons, 1911; Kernan, 1916). The hypoglossal nerve passes through a foramen in the cartilaginous exocciput; this foramen is large during the cartilaginous stage but become smaller with ossification. In front of the rostral end of the notochord, which also marks the rostral border of the parachordal plates, chondrification occurs in the prechordal cartilage and its appendages (Parsons, 1911).

In an embryo of 20 mm CRL (eighth week of gestation), the basichondrocranium is composed of four regions; occipital, otic, orbitotemporalis, and ethmoidal (Kernan, 1916). The following account of basichondrocranial development is derived from Kernan's study. The central portion of the basichondrocranium comprises two continuous ventral and dorsal bars marked by a transverse crest between them (Fig. 6). The transverse crest is the primordium of the dorsum sellae. The dorsal cartilaginous bar is the chordal (basal) plate and the ventral bar is the prechordal plate. The cartilaginous otic capsule is fused with the lateral border of the basal plate, and the line of fusion is marked as the basicapsular commissure or sulcus. The caudal end of the basal plate marks the anterior margin of the foramen magnum. Ventrally, each exoccipital plate is composed of two cranial and caudal roots with an intervening foramen through which the hypoglossal nerve travels. These roots represent the pedicles (neural arches) of the occipital vertebrae. Dorsally, the two roots unite to form a single flat cartilaginous plate known as the exoccipital wing. The lateral border of the exoccipital plate is ventrally separated from the otic capsule by the jugular foramen and is dorsally fused with it at the capsulooccipital commissure. At its posterior border, the exoccipital wing joins a thin plate of triangular cartilage known as the parietal plate of the occipital bone, the apex of which is pointed anteriorly toward the otic capsule. The inferior border of the parietal plate fuses with the otic capsule anteriorly and the exoccipital wing posteriorly. Its superior border is free. From the upper part of the posterior border of the parietal plate, a narrow band of cartilage extends from either plate dorsally and fuses with the contralateral counterpart to form a thin ribbon of cartilage known as the tectum synoticum of "Kernan" or tectum cranii anterius of "Fawcett" (Fig. 6). At this stage, the basichondrocranium contains a very large foramen magnum.

The later stages in basichondrocranial development are prominently characterized by development in the posterior occipital region between the parietal plates and exoccipital wings of both sides. This region

corresponds to the cartilaginous supraoccipital part of the occipital squamous bone. As indicated by the arrows in Figure 6, the parietal plates (below the tectum synoticum) and exoccipital wings of the right and left sides extend dorsomedially, ultimately fusing in the dorsal midline to form a wide, trapezoidal cartilaginous plate posterior to the foramen magnum, known as the tectum posterius of "Kernan" or tectum cranii posterius of "Fawcett." Simultaneously, the tectum synoticum undergoes regression. This view has been supported by Levi (1899), Macklin (1921), and Kernan (1916), and more recently by Müller and O'Rahilly (1980). With regression of the tectum synoticum, the parietal plate simultaneously shrinks (Kernan, 1916). The posterior aspect of the basichondrocranium and occipital region in a fetus of 43 mm CRL (approximately twelfth week of fetal life) is shown in Figure 7. The final fate of the parietal plate of the occipital bone is not well described in the literature, but is most likely retained as the mastoid fontanelle and gives rise to the superolateral part of the cartilaginous supraocciput next to the fontanel. In fact, it has been shown that the mendosal fissure, which postnatally is connected to the mastoid fontanelle, is the remnant of the tectum synoticum of the parietal plate (Niida et al., 1992). Figure 8 shows the mastoid fontanelle and its relationship to the supraocciput and exocciput at birth. The different components of the posterior basichondrocranium and their relationships are schematized in Figure 9.

By the 14th week of gestation, the basichondrocranium achieves its complete maturation (Fig. 10) and endochondral ossification has already been initiated in several other centers (Schäfer et al., 1908; Friede, 1981). Ossification of the cartilaginous basicranium occurs sequentially and in a consistent direction (Kjaer 1990). The first ossification centers in the supraoccipital, exoccipital and basioccipital regions appear in 30, 37, and 51 mm CRL embryos, respectively (Lang, 2001). There is one ossification center in the basioccipital and exoccipital segments; however, the supraoccipital segment develops from multiple ossification centers (Mall, 1906). Radiographically, the ossified basiocciput is easily recognizable when the fetus attains a CRL of 80–100 mm (Kjaer 1990), as is the basisphenoid and anterior basicranium in fetuses of 100 to 150 mm CRL (Kjaer 1990). During the second trimester, the rate of longitudinal growth of the posterior basicranium is approximately half of that of the anterior basicranium (Jeffery, 2002a). Details of the development of the anterior basicranium are beyond the scope of this review.

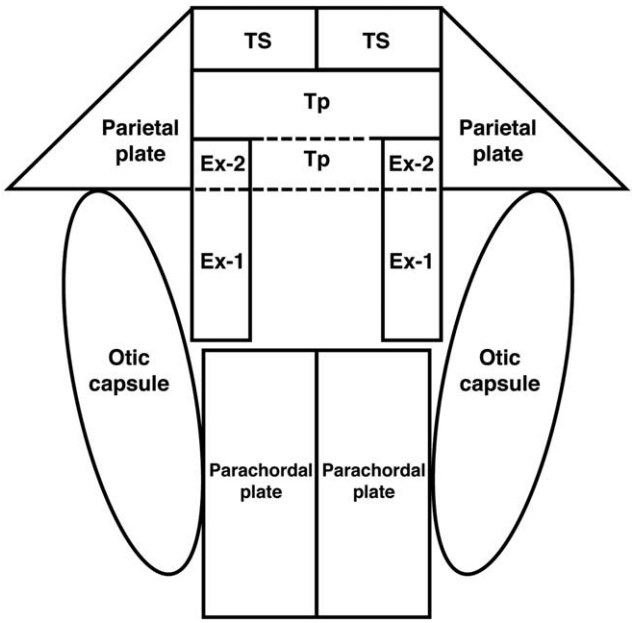

Fig. 9. A schematic drawing of the posterior basichondrocranium. The parachordal plates fuse to form a single basal plate. The exocciput is composed of a root (Ex-1) and a wing (Ex-2). The otic capsule is located lateral to the exocciput and basal plate. Note this schema is a simplified drawing and lacks some details of the anatomical relationships between the related parts. The tectum synoticum (TS), which is a temporary structure, originates from the upper part of the base of the parietal plate. The tectum posterius (TP) originates from the lower part of the base of the parietal plate and exoccipital wing.

CONTRIBUTION OF CELLS OF NEURAL CREST ORIGIN TO THE BASICRANIUM

In their inspirational work, McBratney-Owen and colleagues (2008) demonstrated that the basicranial mesenchyme that is both rostral and caudal to the sphenooccipital synchondrosis is derived from neural crest and mesoderm, respectively, in a mouse model (Fig. 11). The sphenooccipital synchondrosis is initially of dual origin, its rostral half being from the neural crest-derived prechordal cartilage and its caudal half from the mesoderm-derived basiocciput (McBratney-Owen et al., 2008). After birth, the neural crest-derived cells in the synchondrosis vanish and the synchondrosis becomes entirely mesodermal. Later, the mesoderm-derived osteoblasts are brought into the caudal basisphenoid through endochondral ossification of the sphenooccipital synchondrosis (McBratney-Owen et al., 2008). The boundary of the neural crest- and mesoderm-derived basicranium—only roughly correlating with the prechordal-chordal boundary—is ontogenetically and phylogenetically important as it marks the transition from the mesoderm-derived basicranium (posteriorly) to the neural crest-derived basicranium anteriorly. Since they contribute to the formation of the head including the basicranium, cells of neural crest origin could have been predominant in the evolution of vertebrates from chordate-like ancestors (Gans and Northcutt, 1983).

DEVELOPMENT OF THE OCCIPITAL BONE

At birth, the occipital bone comprises a squamous portion and a basioccipital and two exoccipital segments (Fig. 12). The developmental anatomy of the

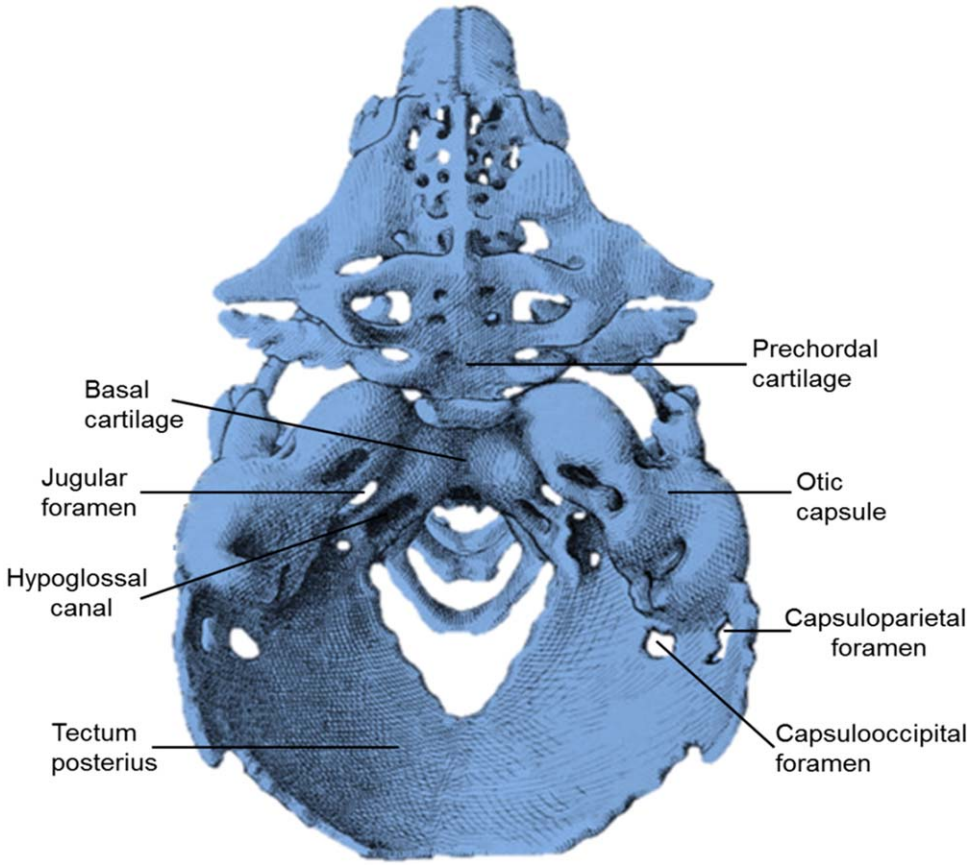

Fig. 10. The superior aspect of the basicranium in a fetus of 80 mm CRL, ~14th week of fetal life (reproduced with slight modifications from Hertwig, 1906). The jugular foramen is located between the otic capsule and exocciput. Two other foramina are visible, one between the otic capsule and the tectum posterius (capsulooccipital foramen) and one between the otic capsule and the parietal plate (capsuloparietal foramen). These foramina transmit emissary veins. They disappear or are retained as the mastoid foramina in adults. [Color figure can be viewed at wileyonlinelibrary.com]

basioccipital and exoccipital segments has been discussed previously. The squamous portion is derived from a lower cartilaginous plate (the origin of this plate from the parietal plates and exoccipital wings has been discussed) and an upper membranous part. The upper membranous part comprises ribbon-like intermediate and triangular interparietal segments (Fig. 13). The membranous interparietal segment is formed by two medial and two lateral plates, one on either side of the midline, in which the medial plates are separated by a median fissure (Srivastava, 1992; Choudhary et al., 2010). Each plate as well as the intermediate segment has two ossification centers (Srivastava, 1992). At 12–15 weeks of gestation, the lateral plates of the membranous interparietal region grow medially and fuse together to form a single hybrid between the intermediate segment below and the medial plates of the interparietal segment above (Shapiro and Robinson, 1976; Srivastava, 1992). A transverse occipital fissure separates the intermediate from the interparietal segment. Subsequently, the transverse fissure is obliterated medially by the fusion of the intermediate and interparietal segments and is thereafter called the lateral (or mendosal) fissure, which is distinguishable at 16 weeks of gestation (Srivastava, 1992). At this time, the median fissure mostly disappears as the two medial plates fuse (Srivastava, 1992).

In a developed skull, the highest nuchal line signifies the border between the intermediate segment and interparietal bone, whereas the superior nuchal line represents the border between the intermediate segment and the cartilage-derived supraocciput. Initially, the lateral fissure transforms into a suture (mendosal suture) at the lateral part of the highest nuchal line. With complete fusion of bones, the mendosal suture normally disappears between the second and fourth years of life. If this does not occur, the mendosal suture can persist, as reported in 16% of adult skulls (Tubbs et al., 2007). Very rarely, the entire transverse fissure/suture between the intermediate and interparietal segments can persist; this should not be confused with the mendosal suture (Lochmuller et al., 2011). It should be noted here that

the terms "fissure" and "suture" are often used interchangeably, some authors favoring one over the other (Balboni et al., 2005). In a morphological sense, they are different stages of the same structure; ontogenetically, the fissure is replaced by the suture, and the suture can be completely obliterated following ossification.

The appearance of ossification centers in the supraoccipital cartilage has long been controversial. According to Mall (1906), two paramedian ossification centers appear in the 55-day-old embryo and these speedily fuse into a single median center. Simultaneously, two new ossification centers appear lateral to the fusing paramedian centers, to which they also join by Day 57. Therefore, on Day 58, there is a single ossifying mass across the supraoccipital midline. As mentioned earlier, the supraoccipital cartilage can be arbitrarily divided into a central plate and two lateral plates (Fig. 7). The paramedian centers occupy the central plate and lateral centers occupy the upper parts of the lateral plates (Srivastava, 1977). Srivastava (1977) also mentions another independent ossification center in the lower part of the lateral plate of the supraoccipital cartilage on either side. The different segments and plates of the developing supraoccipital squama are schematized in Figure 13. The rapid formation and fusion of the supraoccipital ossification centers could account for the discrepancies in the literature regarding the number and arrangement of those centers.

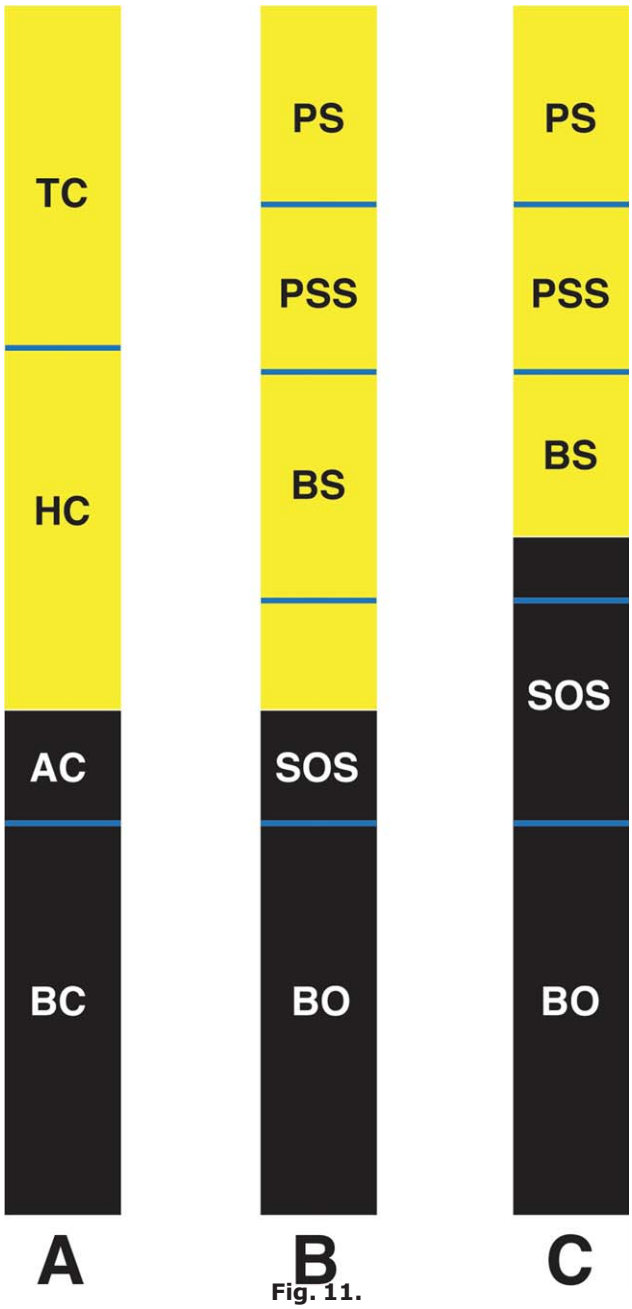

Fig. 11.

BASICRANIAL ANGLE, PLATYBASIA AND BASILAR KYPHOSIS

The basal angle is formed between the axes of the anterior and posterior basicranium. For practical purposes, the center of the pituitary fossa (Koenigsberg et al., 2005), tuberculum sellae (Schady et al., 1987; Jeffery, 2005), or dorsum sellae (Koenigsberg et al., 2005) is used as a landmark for the basicranial hinge around which the posterior basicranium rotates. The basion is invariably used as the inferior limit of the posterior basicranium (Schady et al., 1987; Jeffery, 2005; Koenigsberg et al., 2005), and the foramen cecum (Jeffery, 2002b, 2005) or nasion (Koenigsberg et al., 2005) is used as the front limit of the anterior basicranium. Figure 14 shows different landmarks and methods used for measuring the basicranial angle. The posterior basicranium retroflexes during the fetal period, increasing the basicranial angle (Jeffery, 2002b, 2005; Jeffery and Spoor, 2002). This retroflexion moves the basion dorsally and superiorly, flattens the basicranium (Jeffery and Spoor, 2002) and decreases the ventral depth of the posterior cranial

Fig. 11. Dynamic changes in the boundary of the neural crest- and mesoderm-derived basicranium based on a mouse model (reproduced, with permission from Elsevier, from McBratney-Owen et al., (2008) with modifications). AC, acrochordal cartilage; BC, basal cartilage; BO, basiocciput; BS, basisphenoid; HC, hypophyseal cartilage; PS, presphenoid; PSS, presphenoidal synchondrosis; TC, trabecular cartilage; SOS, sphenooccipital synchondrosis. **A**, the fetal period. The acrochordal cartilage is the rostral part of the basal cartilage surrounding the tip of the notochord. The black region is a mesodermal derivative and the yellow region is a neural crest derivative. **B**, the early postnatal period. Note that the sphenooccipital synchondrosis has a dual origin. **C**, the late postnatal period. With apoptosis of neural crest cells and introduction of mesoderm-derived osteoblasts into the caudal basisphenoid, the mesoderm-neural crest boundary moves anteriorly. The entire sphenooccipital synchondrosis is now mesodermally derived. [Color figure can be viewed at wileyonlinelibrary.com]

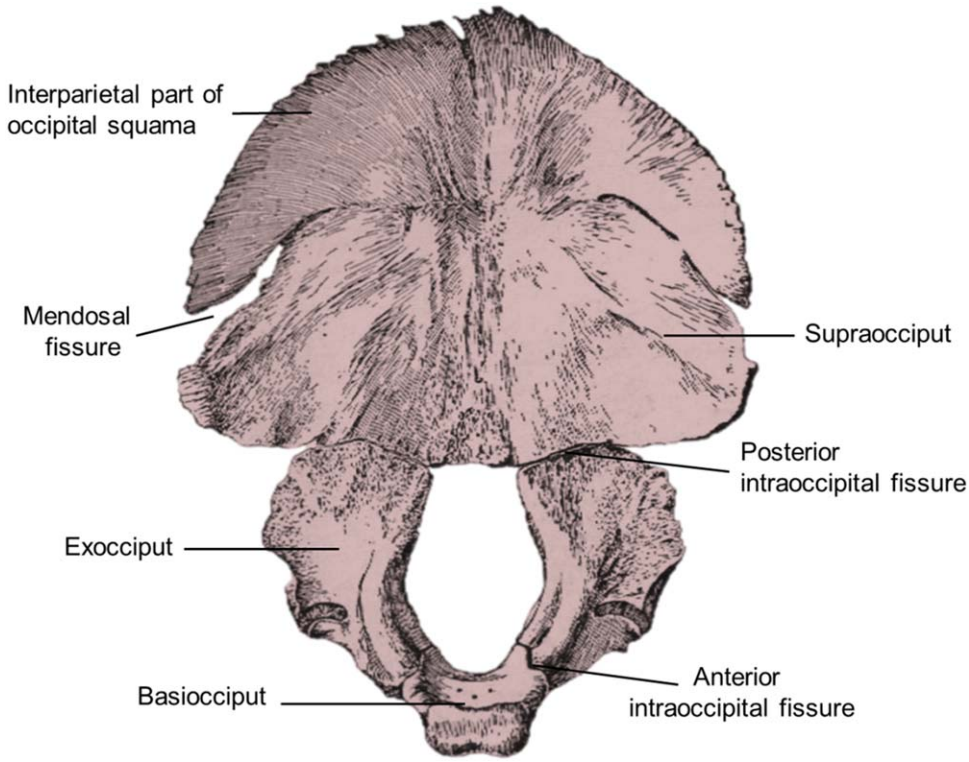

Fig. 12. The occipital bone at birth (after Piersol, 1918). [Color figure can be viewed at wileyonlinelibrary.com]

fossa. There are two hypotheses about the mechanism of posterior basicranial retroflexion: enlargement of the intracranial space and, more importantly, expansion of the developing upper airways, which can act from above and below to flatten the skull base (Jeffery and Spoor, 2002; Jeffery, 2005). Excessive retroflexion of the posterior basicranium results in platybasia, whereas insufficient retroflexion results in basilar kyphosis. The normal angle varies slightly depending on the method and landmarks used for its measurement. An angle between 125° and 143° is generally considered normal (Koenigsberg et al., 2005). A basicranial angle $>143°$ indicates platybasia and one $<125°$ indicates basilar kyphosis (Koenigsberg et al., 2005). Isolated and mild platybasia is asymptomatic and affects the posterior fossa volume insignificantly (Hodak et al., 1998). Moderate to severe platybasia is often associated with basilar invagination (Smoker, 1994). The basicracranial angle is greater in patients with Chiari I malformation (Schady et al., 1987).

BASILAR INVAGINATION AND BASILAR IMPRESSION

Basilar invagination occurs when the caudal part of the occipital bone is displaced inward and upward, and the vertebral column and skull base abnormally approximate each other. It is one of the most common anomalies of the craniovertebral junction. In severe cases, the odontoid process is prolapsed into the foramen magnum (Schady et al., 1987). Basilar invagination can be congenital or secondary to such conditions as Paget's disease, osteogenesis imperfecta, hyperparathyroidism, rickets, and so forth (Smoker, 1994). The secondary or acquired forms of basilar invagination are referred to as basilar impression (Smoker, 1994). The congenital forms are associated with hypoplasia of the atlas, basiocciput, and/or occipital condyle, platybasia and atlantooccipital assimilation (Bares, 1975; Smoker, 1994) and a higher incidence of hindbrain herniation (Bares, 1975; Schady et al., 1987). Such associations do not necessarily reflect a cause-effect relationship in all cases. Instead, they can represent consequences of the same pathological mechanism. The craniocervical growth collision theory of Roth is worth mentioning here as a potential embryological explanation for the occurrence of basilar invagination and associated anomalies. According to Roth (1986), following an early embryonic period of predominant neural growth, the proliferation of skeletogenic tissue and vertebral growth ultimately overtake the growth of the spinal cord. Normally, the vertebral column grows in a cranio-caudal direction resulting in expansion of the vertebrae below the distal end of the spinal cord. If the distribution of skeletogenic tissue is reversed for any reason and vertebral growth occurs in a caudo-cranial direction, the growing vertebral column collides with the developing skull

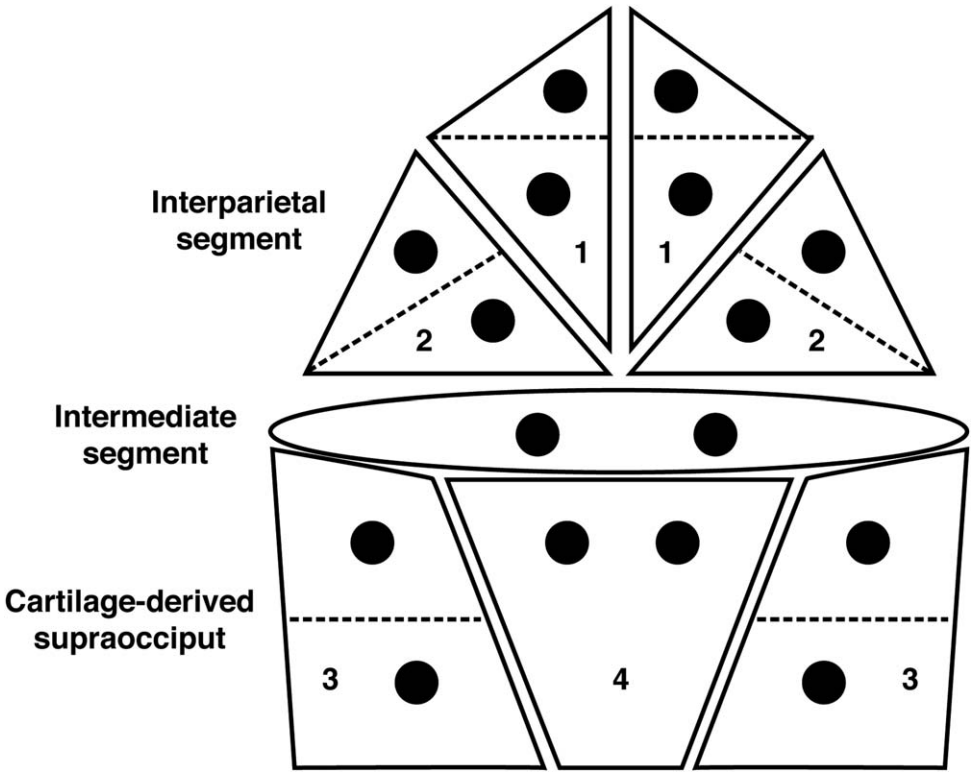

Fig. 13. A line diagram showing the different segments contributing to the development of the squamous portion of the occipital bone and their respective ossification centers. **1**, medial plates of the interparietal segment; **2**, lateral plates of the interparietal segments; **3**, lateral plates of the supraoccipital cartilage; **4**, central plate of the supraoccipital cartilage. The intermediate segment and cartilage-derived supraocciput together form the supraoccipital part of the occipital squama. The ossification centers are indicated by black circles. The dashed lines represent the boundaries between them. The variable separation and fusion of the different plates and/or ossification centers can result in the formation of variant sutures and sutural (inca) bones in the adult skull (Choudhary et al., 2010).

base (Roth, 1986). This collision will push the posterior skull base and the margin of the foramen magnum upward and compress the primordia of the occipital and cervical vertebrae against each other, potentially leading to abnormal segmentation at the craniovertebral junction, fusion of the atlas and occipital bones, platybasia, and prolapse of cervical vertebral column into the skull base.

There are several morphometric criteria for diagnosing basilar invagination (Hinck et al., 1961). Figure 15 shows some of the reference lines used for this purpose. Basilar invagination is divided into two groups, one without (Group 1) and one with (Group 2) associated Chiari I malformation (Goel et al., 1998; Pearce, 2007). Currently, only about 20% of patients with basilar invagination have Chiari malformation (Pearce, 2007). Pure basilar invagination has pyramidal motor and proprioceptive deficits, whereas basilar invagination with Chiari malformation usually presents chronically with cerebellar and vestibular deficits (Caetano de Barros et al., 1968; Goel et al., 1998). A familial form of basilar invagination has been reported and an autosomal dominant pattern of inheritance with incomplete penetrance and variable expressivity was suggested for this case (Paradis and Sax, 1972).

SHALLOWNESS OF THE POSTERIOR CRANIAL FOSSA IN CHIARI I MALFORMATION

Various linear morphometric measurements have been defined to determine the dimensions and size of the posterior cranial fossa and occipital bone (Fig. 16). In a study comparing the depths of the posterior cranial fossa among Chiari I patients aged over 15 years with normal controls, the height of the supratentorial occipital region (H) was similar in the two groups (Karagöz et al., 2002). However, the posterior fossa height or depth (h) was approximately 16% less among the Chiari 1 patients. This observation, which has been confirmed in several other studies (Schady et al., 1987; Greenlee et al., 1999), implies that patients with Chiari I malformation have a shallow posterior fossa. As the supratentorial and infratentorial

Fig. 14. Midsagittal magnetic resonance imaging of the head. The different landmarks used for measuring the basicranial angle are shown. 1, nasion; 2, foramen cecum; 3, tuberculum sellae; 4, center of pituitary fossa; 5, dorsum sellae; 6, basion; 7, opisthion. Note the opisthion-basion-tuberculum sellae angle is known as Boogard's angle. The size of the posterior cranial fossa decreases with an increase in Boogard's angle (Schady et al., 1987).

parts of the squamous occipital bone are composed of membranous and cartilaginous origins, respectively, the shallowness of the posterior fossa reflects an abnormality of the occipital squamous bone restricted to its cartilage-derived lower part.

UNDERDEVELOPMENT OF THE OCCIPITAL BONE AND BASIOCCIPITAL HYPOPLASIA IN CHIARI I MALFORMATION

Nishikawa et al. (1997) compared the occipital bone morphometry among patients aged 15 years and older with Chiari I malformation, and to healthy age- and gender-matched controls. The supraocciput and exoccipital heights (measured from the jugular tubercle to the atlantooccipital joint) were ~20% lower in patients with Chiari I malformation. In another study, Noudel et al. (2009) compared the basioccipital lengths (measured from the sphenooccipital synchondrosis to the basion) among 17 patients with Chiari I malformation aged over 16 years with healthy controls. The basioccipital length was also lower among Chiari I patients. The association of a short clivus with Chiari I malformation has been confirmed by other studies (Vega et al., 1990; Karagöz et al., 2002). The bulk of evidence indicates that the supraoccipital, exoccipital and basioccipital segments of the occipital bone are underdeveloped and hypoplastic, albeit to various degrees, in Chiari I malformation (Cesmebasi et al., 2015). Severe basioccipital hypoplasia or dysgenesis is associated with basilar invagination (Nishikawa et al., 1997). Dysgenesis of the basiocciput can be associated with a normal-appearing basisphenoid (Shah and Goel, 2010). Basioccipital dysgenesis (with scalloping, concavity, and thinness) has also been reported in the Chiari II malformation (Schady et al., 1987).

NOLINEAR NATURE OF OCCIPITAL BONE DYSPLASIA IN CHIARI I MALFORMATION

In order to elucidate the nature of occipital bone dysplasia in Chiari I malformation, a meta-analysis was performed. Figure 17 shows the results of this meta-analysis for four studies that reported the means and standard deviations of clival or supraoccipital length or size of the foramen magnum in adult patients with Chiari I malformation (Milhorat et al., 1999; Karagöz et al., 2002; Aydin et al., 2005; Dufton et al., 2011). Although there were significant reductions in the lengths of the supraocciput and clivus, the meta-analysis indicated that the overall size reduction is more prominent in the supraocciput than in the clivus. This is consistent with the observations by Nishikawa et al. (1997) and Dagtekin et al. (2011) on adult Chiari I patients in whom the supraocciput was significantly more underdeveloped than the clivus. The meta-analysis also indicated a tendency for the foramen magnum to widen anteroposteriorly; however, this increase in foramen magnum size was not proportionate to the retardation of the supraocciput and clivus. Overall, it seems that occipital bone dysplasia in Chiari I malformation is nonlinear and different parts of this bone are disproportionately affected.

To recap, the supraocciput develops through a morphologically complex process of chondrification and ossification. The chondrified supraocciput is derived from the parietal plate and exocciput, and is composed of lateral and central plates. The lateral plates ossify by two upper and lower ossification centers and the central plate by two centers that rapidly fuse. The parietal plate undergoes partial reversion during fetal life, rendering the upper part of the chondrified supraocciput derived from this plate also vulnerable to regression. This could potentially provide an embryological basis for the shortening of the supraocciput in Chiari malformation.

MIDFACE RETROCESSION IN CHIARI MALFORMATION

In an experimental fetal animal model of Chiari malformations and spinal dysraphism induced by a single maternal dose of vitamin A, Marin-Padilla and

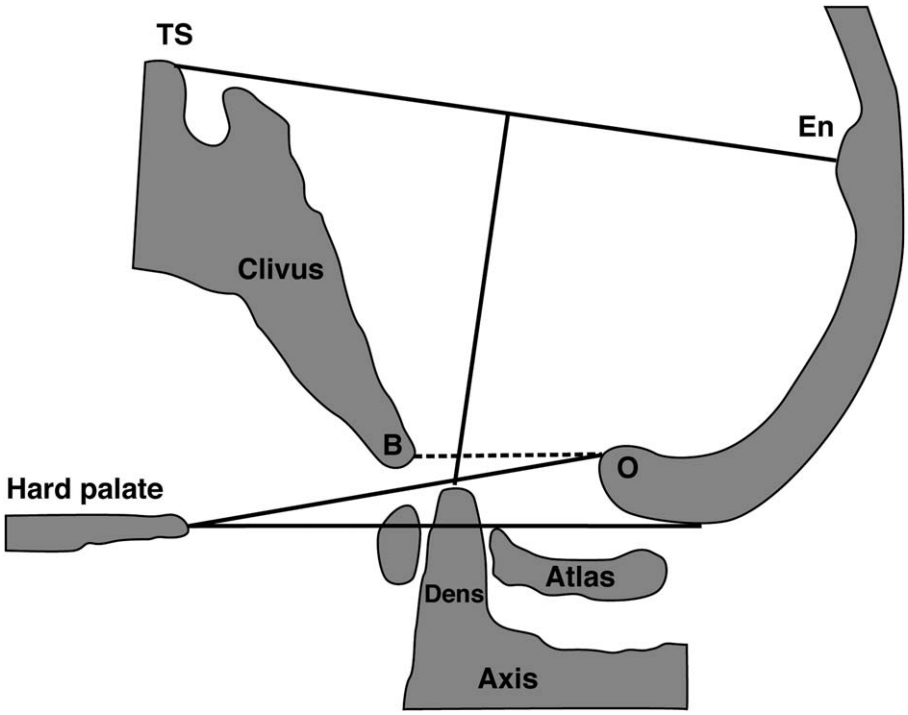

Fig. 15. Reference lines used for diagnosing basilar invagination. Chamberlain's line connects the posterior end of the hard palate to the opisthion (O). McGregor's line extends from the posterior end of the hard palate to the lowest point on the midline supraoccipital curve (Hinck et al., 1961; Smith et al., 2010). Note the posterior margin of the foramen magnum is curved upward into the posterior cranial fossa, which is usually the case in basilar invagination. McRae's line extends from the basion (B) to the opisthion (O). Twining's line connects the tuberculum sellae (TS) and the endinion (En). A line perpendicular to Twining's line, which passes through the apex of the dens, is the Klaus height index line (Hinck et al., 1961). Normally, the apex of the dens should lie below McRae's line (Smith et al., 2010). Severe basilar invagination is diagnosed when the odontoid process violates McRae's line. The diagnosis of basilar invagination is considered if the odontoid process extends beyond 5 mm and 7 mm above Chamberlain's and McGregor's lines, respectively (Smith et al., 2010). A Klaus height index $<$30 mm indicates basilar invagination and a value between 30 and 36 mm indicates a tendency toward basilar invagination (Hinck et al., 1961). It should be mentioned that opinions differ on the cutoff value of those diagnostic measurements.

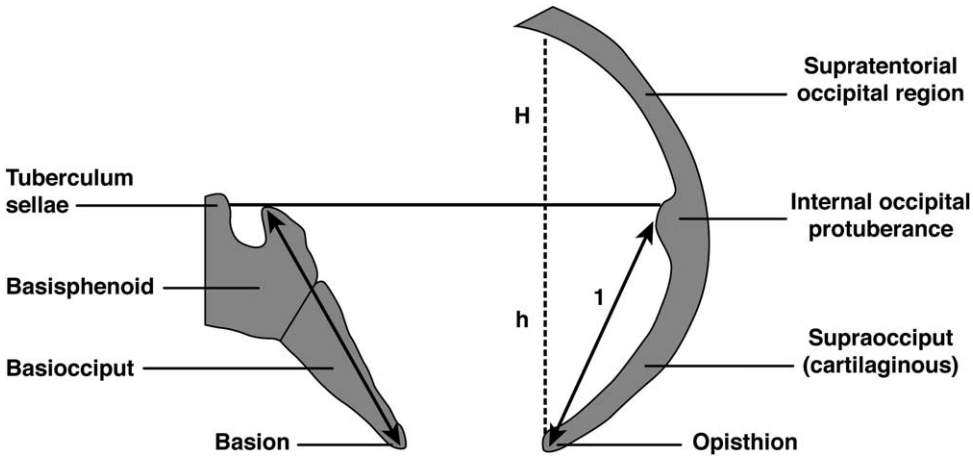

Fig. 16. Linear morphometry of the posterior cranial fossa and occipital bone. McRae's and Twining's lines are shown. A line perpendicular to Twining's line is drawn at one quarter of its distance from the endinion (internal occipital protuberance) connecting the inner table of bones in the infra- and supra-tentorial compartments. The distances between Twining's line and the inner table of the skull in the supratentorial and infratemporal regions respectively indicate the depth of the posterior fossa in the supraoccipital region and the height of the supratentorial occipital region (Krogness, 1978; Karagöz et al., 2002). The lengths of the supraocciput and clivus are represented by the two-headed arrows 1 and arrow parallel to the clivus, respectively.

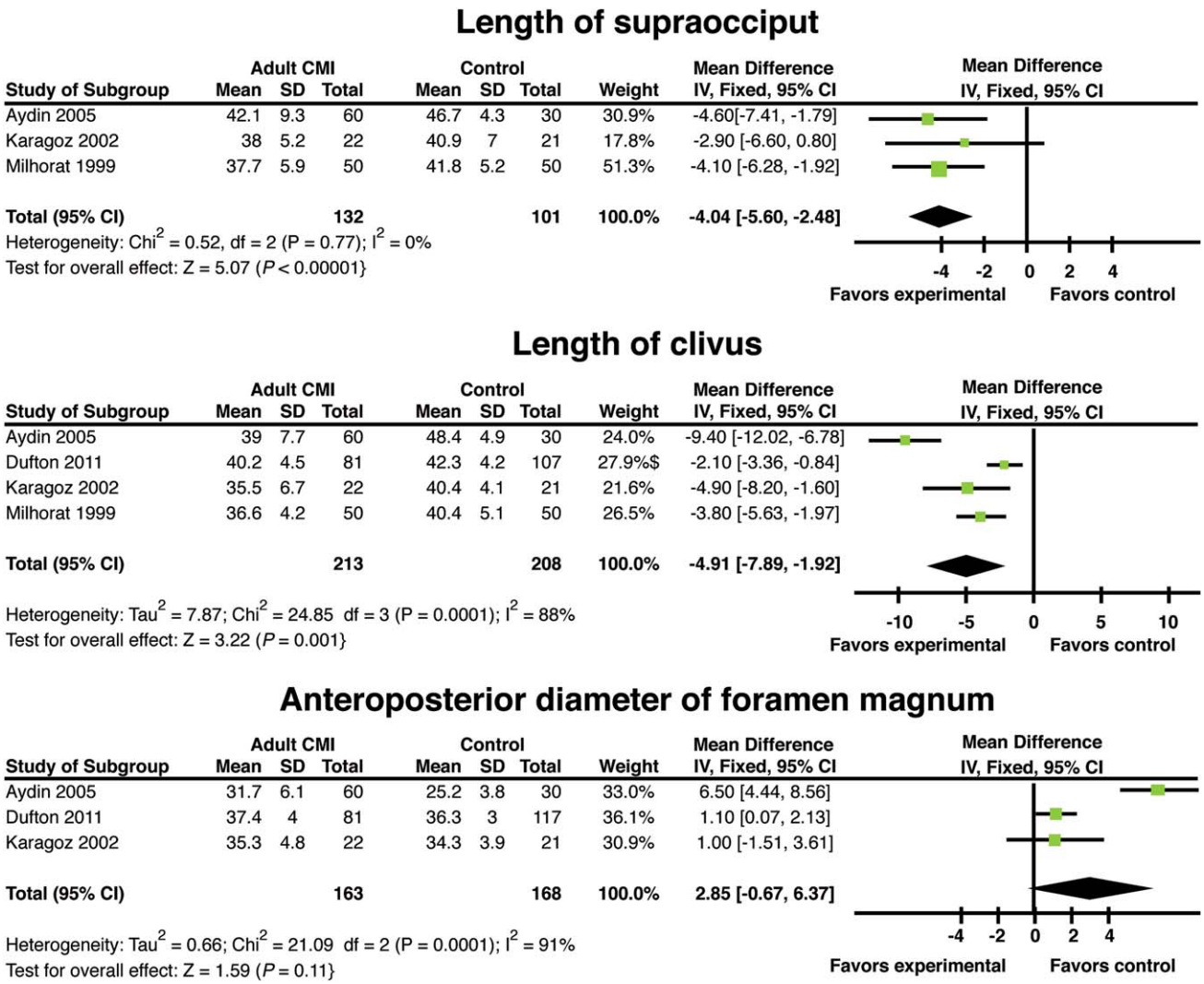

Fig. 17. Forest plots comparing the clival and supraoccipital lengths and anteroposterior diameter of the foramen magnum among adult patients with Chiari I malformation and controls. Homogeneity-based meta-analysis was performed using Review Manager Version 5 for Windows (Cochrane Collaboration and Update Software). Homogeneity between studies was assessed using the standard Cochran's Q and I^2 statistics. A fixed effect model (for a data set with non-significant heterogeneity) or random effect model (for a data set with significant heterogeneity) was used to merge odds ratio values and to estimate the overall effect size. Overall effect, odds ratios and confidence intervals are presented. [Color figure can be viewed at wileyonlinelibrary.com]

Marin-Padilla (1981) noted that underdevelopment of the occipital bone and posterior cranial fossa causes the maxilla to take a more posterior position within the viscerocranium, leading to retrocession of the midface. In humans, a subtle midface retrocession can best be evaluated by the length of Chamberlain's line; a short Chamberlain's line reflects midface retrocession with respect to the occipital region. Chamberlain's line is shorter in patients with Chiari I malformation, reflecting a subtle abnormality in the midface (Schady et al., 1987). Interestingly, patients with greater midface retrocession have smaller posterior fossae (Schady et al., 1987). Further studies are required to elucidate the potentially more pervasive, albeit subtle, abnormalities of the viscerocranium among Chiari patients.

CONCLUSIONS

The embryology of the posterior cranial fossa is complex and relies on a unique timing of various neurovascular and bony elements. Derailment of these developmental processes can lead to a wide range of malformations such as the Chiari malformations. Therefore, a good working knowledge of this embryology is important for those treating patients with involvement of this region of the cranium.

REFERENCES

Allen W. 1879. The Varieties of the atlas in the human subject, and the homologies of its transverse processes. J Anat Physiol 14: 18–27.

Anderson T. 1996. Paracondylar process: Manifestation of an occipital vertebra. Int J Osteoarchaeo 6:195–201.

Aydin S, Hanimoglu H, Tanriverdi T, Yentur E, Kaynar MY. 2005. Chiari type I malformations in adults: A morphometric analysis of the posterior cranial fossa. Surg Neurol 64:237–241.

Bailey RW, Sherk HH, Dunn EJ. (eds.) 1983.The Cervical Spine - The Cervical Spine Research Society. Philadelphia: JB Lippincott.

Balboni AL, Estenson TL, Reidenberg JS, Bergemann AD, Laitman JT. 2005. Assessing age-related ossification of the petro-occipital fissure: Laying the foundation for understanding the clinicopathologies of the cranial base. Anat Rec 282:38–48.

Bares L. 1975. Basilar impression and the so-called 'associated anomalies'. Eur Neurol 13:92–100.

Bergman RA, Afifi AK, Miyauchi R. 1996. Cervical vertebrae. URL: http://www.anatomyatlases.org/AnatomicVariants/SkeletalSystem/Text/CervicalVertebrae.shtml [accessed February 2012].

Burke AC, Nelson CE, Morgan BA, Tabin C. 1995. Hox genes and the evolution of vertebrate axial morphology. Development 121: 333–346.

Caetano de Barros M, Farias W, Ataide L, Lins S. 1968. Basilar impression and Arnold-Chiari malformation. A study of 66 cases. J Neurol Neurosurg Psychiatry 31:596–605.

Caffey J. 1953. On the accessory ossicles of the supraoccipital bone: Some newly recognized roentgen features of the normal infantile skull. Am J Roentgenol Radium Ther Nucl Med 70:401–412.

Cankal F, Ugur HC, Tekdemir I, Elhan A, Karahan T, Sevim A. 2004. Fossa navicularis: Anatomic variation at the skull base. Clin Anat 17:118–122.

Cesmebasi A, Loukas M, Hogan E, Kralovic S, Tubbs RS, Cohen-Gadol AA. 2015. The Chiari malformations: A review with emphasis on anatomical traits. Clin Anat 28:184–194.

Chopra JS, Sawhney IM, Kak VK, Khosla VK. 1988. Craniovertebral anomalies: A study of 82 cases. Br J Neurosurg 2:455–464.

Choudhary AK, Jha B, Boal DK, Dias M. 2010. Occipital sutures and its variations: The value of 3D-CT and how to differentiate it from fractures using 3D-CT? Surg Radiol Anat 32:807–816.

Christ B, Huang R, Scaal M. 2004. Formation and differentiation of the avian sclerotome. Anat Embryol (Berl) 208:333–350.

Condie BG, Capecchi MR. 1993. Mice homozygous for a targeted disruption of Hoxd-3 (Hox-4.1) exhibit anterior transformations of the first and second cervical vertebrae, the atlas and the axis. Development 119:579–595.

Csakany G. 1957. Proatlas manifestation as diagnostic problem [Hungarian]. Magy Radiol 9:216–220.

Dagtekin A, Avci E, Kara E, Uzmansel D, Dagtekin O, Koseoglu A, Talas D, Bagdatoglu C. 2011. Posterior cranial fossa morphometry in symptomatic adult Chiari I malformation patients: Comparative clinical and anatomical study. Clin Neurol Neurosurg 113: 399–403.

Davies HW. 1967. Radiological changes associated with Arnold-Chiari malformation. Br J Radiol 40:262–269.

Denisov SD, Kabak SL. 1984. Rare case of manifestation of a proatlas [Russian]. Arkh Anat Gistol Embriol 86:75–77.

Dockter JL. 2000a. Sclerotome induction and differentiation. Curr Top Dev Biol 48:77–127.

Dockter JL. 2000b. Sclerotome induction and differentiation. In: Ordahl CP, editor. Somitogenesis: Part 2. San Diego: Academic Press. p 77–128.

Dufton JA, Habeeb SY, Heran MK, Mikulis DJ, Islam O. 2011. Posterior fossa measurements in patients with and without Chiari I malformation. Can J Neurol Sci38 (38:):452–455.

Ebensperger C, Wilting J, Brand-Saberi B, Mizutani Y, Christ B, Balling R, Koseki H. 1995. Pax-1, a regulator of sclerotome development is induced by notochord and floor plate signals in avian embryos. Anat Embryol (Berl) 191:297–310.

Fan CM, Tessier-Lavigne M. 1994. Patterning of mammalian somites by surface ectoderm and notochord: Evidence for sclerotome induction by a hedgehog homolog. Cell 79:1175–1186.

Ferrier DE, Holland PW. 2001. Ancient origin of the Hox gene cluster. Nat Rev Genet 2:33–38.

Finke J. 1964. On the incidence of the pharyngeal tubercle, a roentgenological variant at the base of the skull [German]. Dtsch Z Nervenheilkd 186:186–189.

Frazer JE. 1931. A manual of Embryology. New York: William Wood and Company. p 142–163.

Friede H. 1981. Normal development and growth of the human neurocranium and cranial base. Scand J Plast Reconstr Surg 15: 163–169.

Ganguly DN, Roy KK. 1964. A study on the cranio-vertebral joint in the man. Anat Anz Bd 114:433–452.

Gans C, Northcutt RG. 1983. Neural crest and the origin of vertebrates: A new head. Science 220:268–273.

Gasser RF. 1976. Early formation of the basicranium in man. In: Bosma JF, editor. Symposium on Development of the Basicranium. Bethesda: Department of Health, Education and Welfare. p 29–43.

Gholve PA, Hosalkar HS, Ricchetti ET, Pollock AN, Dormans JP, Drummond DS. 2007. Occipitalization of the atlas in children. Morphologic classification, associations, and clinical relevance. J Bone Joint Surg Am 89:571–578.

Gladstone RJ, Erichsen-Powell W. 1915. Manifestation of occipital vertebrae, and fusion of the atlas with the occipital bone. J Anat Physiol 49:190–209.

Goel A, Shah A. 2010. Unusual bone formation in the anterior rim of foramen magnum: Cause, effect and treatment. Eur Spine J 19: S162–S164.

Goel A, Bhatjiwale M, Desai K. 1998. Basilar invagination: A study based on 190 surgically treated patients. J Neurosurg 88:962–968.

Greenlee J, Garell PC, Stence N, Menezes AH. 1999. Comprehensive approach to Chiari malformation in pediatric patients. Neurosurg Focus 6:e4.

Halanski MA, Iskandar B, Nemeth B, Noonan KJ. 2006. The coconut condyle: Occipital condylar dysplasia causing torticollis and leading to c1 fracture. J Spinal Disord Tech 19:295–298.

Hauser G, De Stefano GF. 1989. Epigenetic Variants of the Human Skull. Stuttgart: Schweizerbartsche

Hertwig O. 1906. Handbuch Der Vergleichenden Und Experimentellen Entwicklungslehre Der Wirbeltiere, Band II, Teil 2. Jena: G. Fischer 824.

Hinck VC, Hopkins CE, Savara BS. 1961. Diagnostic criteria of basilar impression. Radiology 76:572–585.

Hodak JA, Mamourian A, Dean BL. 1998. Radiologic evaluation of the craniovertebral junction. In: Dickman CA, Spetzler RF, Sonntag VK, editors. Surgery of the Craniovertebral Junction. New York: Thiem.

Jeffery N. 2002a. A high-resolution MRI study of linear growth of the human fetal skull base. Neuroradiology 44:358–366.

Jeffery N. 2002b. Differential regional brain growth and rotation of the prenatal human tentorium cerebelli. J Anat 200:135–144.

Jeffery N. 2005. Cranial base angulation and growth of the human fetal pharynx. Anat Rec A Discov Mol Cell Evol Biol 284:491–499.

Jeffery N, Spoor F. 2002. Brain size and the human cranial base: A prenatal perspective. Am J Phys Anthropol 118:324–340.

Johnson GF, Israel H. 1979. Basioccipital clefts. Radiology 133:101–103.

Kalla AK, Khanna S, Singh IP, Sharma S, Schnobel R, Vogel F. 1989. A genetic and anthropological study of atlanto-occipital fusion. Hum Genet 81:105–112.

Karagöz F, Izgi N, Kapíjcíjoğlu Sencer S. 2002. Morphometric measurements of the cranium in patients with Chiari type I malformation and comparison with the normal population. Acta Neurochir (Wien) 144:165–171.

Kassim NM, Latiff AA, Das S, Ghafar NA, Suhaimi FH, Othman F, Hussan F, Sulaiman IM. 2010. Atlanto-occipital fusion: An

osteological study with clinical implications. Bratisl Lek Listy 111: 562–565.
Kernan JD. Jr. 1916. The Chondrocranium of a 20 mm. Human Embryo. J Morphol 27:605–646.
Kjaer I. 1990. Ossification of the human fetal basicranium. J Craniofac Genet Dev Biol 10:29–38.
Koenigsberg RA, Vakil N, Hong TA, Htaik T, Faerber E, Maiorano T, Dua M, Faro S, Gonzales C. 2005. Evaluation of platybasia with MR imaging. AJNR Am J Neuroradiol 26:89–92.
Krogness KG. 1978. Posterior fossa measurements. I. The normal size of the posterior fossa. Pediatr Radiol 6:193–197.
Kruyff E. 1967. Transverse cleft in the basi-occiput. Acta Radiol Diagn (Stockh 6:41–48.
Kunicki J, Ciszek B. 2005. The clinical anatomy and the occipital condyle variants. Clin Anat 18:646–647.
Lakhtakia PK, Premsagar IC, Bisaria KK, Bisaria SD. 1991. A tubercle at the anterior margin of the foramen magnum. J Anat 177:209–210.
Lang J. 2001. Skull Base and Related Structures: Atlas of Clinical Anatomy. 2nd Ed. Stuttgart: Schattauer.
Le Double AF. 1903. Traité des variations des os du crane de l'homme, et de leur signification au point de vue de l'anthropologie zoologique. Paris: Vigot Freres.
Lemire RJ. 2000. Embryology of the skull. In: Cohen MM Jr, MacLean RE, editors. Craniosynostosis. Diagnosis, Evaluation and Management. 2nd Ed. Oxford: Oxford University Press. p 25–34.
Levi G. 1899. Beitrag lum studium der entwickelung des knorpeligen primordialcraniums des menschen. Arch Mikr Anat 55:341–414.
Lochmuller CM, Marks MK, Mileusnic-Polchan D, Cogswell SC. 2011. Misidentification of a transverse occipital suture as a persistent mendosal suture. J Pediatr 159:876–877.
Ludwig KS. 1957. Die frühentwicklung des atlas und der occipitalwirbel beim menschen. Acta Anat (Basel) 30:444–461.
Macalister A. 1893. Notes on the development and variations of the Atlas. J Anat Physiol 27:519–542.
Macklin CC. 1921. The skull of a human fetus of 43 millimeters greatest length. Contrib Embryol 48:57–103.
Madeline LA, Elster AD. 1995a. Suture closure in the human chondrocranium: CT assessment. Radiology 196:747–756.
Madeline LA, Elster AD. 1995b. Postnatal development of the central skull base: Normal variants. Radiology 196:757–763.
Mall FP. 1906. On ossification centers in human embryos less than one hundred days old. Am J Anat 5:433–458.
Marin-Padilla M, Marin-Padilla TM. 1981. Morphogenesis of experimentally induced Arnold–Chiari malformation. J Neurol Sci 50: 29–55.
McBratney-Owen B, Iseki S, Bamforth SD, Olsen BR, Morriss-Kay GM. 2008. Development and tissue origins of the mammalian cranial base. Dev Biol 322:121–132.
Menezes AH. 1995. Primary craniovertebral anomalies and the hindbrain herniation syndrome (Chiari I): Data base analysis. Pediatr Neurosurg 23:260–269.
Menezes AH. 2008. Craniocervical developmental anatomy and its implications. Childs Nerv Syst 24:1109–1122.
Menezes AH, Fenoy KA. 2009. Remnants of occipital vertebrae: Proatlas segmentation abnormalities. Neurosurgery 64:945–953.
Milhorat TH, Chou MW, Trinidad EM, Kula RW, Mandell M, Wolpert C, Speer MC. 1999. Chiari I malformation redefined: Clinical and radiographic findings for 364 symptomatic patients. Neurosurgery 44:1005–1017.
Müller F, O'Rahilly R. 1980. The human chondrocranium at the end of the embryonic period, proper, with particular reference to the nervous system. Am J Anat 159:33–58.
Müller F, O'Rahilly R. 1994. Occipitocervical segmentation in staged human embryos. J Anat 185:251–258.
Müller F, O'Rahilly R. 2003. Segmentation in staged human embryos: The occipitocervical region revisited. J Anat 203:297–315.
Nayak SR, Krishnamurthy A, Madhan Kumar SJ, Prabhu LV, Jiji PJ, Pai MM, Kumar A, Avadhani R. 2007. The mendosal suture of the occipital bone: Occurrence in Indian population, embryology and clinical significance. Surg Radiol Anat 29:329–332.
Niida S, Yamasaki A, Kodama H. 1992. Interference with interparietal growth in the human skull by the tectum synoticum posterior. J Anat 180:197–200.
Nishikawa M, Sakamoto H, Hakuba A, Nakanishi N, Inoue Y. 1997. Pathogenesis of Chiari malformation: A morphometric study of the posterior cranial fossa. J Neurosurg 86:40–47.
Noudel R, Jovenin N, Eap C, Scherpereel B, Pierot L, Rousseaux P. 2009. Incidence of basioccipital hypoplasia in Chiari malformation type I: Comparative morphometric study of the posterior cranial fossa. Clinical article. J Neurosurg 111:1046–1052.
Oetteking B. 1923. On the morphological significance of certain cranio-vertebral variations. Anat Rec 25:339–353.
Ohaegbulam C, Woodard EJ, Proctor M. 2005. Occipitocondylar hyperplasia: An unusual craniovertebral junction anomaly causing myelopathy. Case report. J Neurosurg 103:379–381.
O'Rahilly R, Müller F. 1984. The early development of the hypoglossal nerve and occipital somites in staged human embryos. Am J Anat 169:237–257.
Pang D, Thompson DN. 2011. Embryology and bony malformations of the craniovertebral junction. Childs Nerv Syst 27:523–564.
Paradis RW, Sax DS. 1972. Familial basilar impression. Neurology 22:554–560.
Parsons FG. 1911. Skull. In: Encyclopedia Britannica, Vol. 25, 11th Ed. New York: Encyclopedia Britannica Company. p 196–200.
Pearce JM. 2007. Platybasia and basilar invagination. Eur Neurol 58: 62–64.
Piersol GA. (ed.) 1918. Human Anatomy Including Structure and Development and Practical Considerations. 6th Ed. Philadelphia: J.B. Lippincott Company.
Pourquié O. (ed.) 2009. Hox genes. San Diego: Academic Press.
Prescher A. 1996. The craniocervical junctions and its variations. In: Voger R, Fanghanel J, Giebel J, editors. Aspects of Teratology, Volume 1 - Proceedings on the 9th Teratology Symposium, Greifswald, August 30-September 1, 1995. Marburg: Tectum Verlag. p 62–64.
Prescher A. 1997. The craniocervical junction in man, the osseous variations, their significance and differential diagnosis. Ann Anat 179:1–19.
Prescher A, Brors D, Adam G. 1996. Anatomic and radiologic appearance of several variants of the craniocervical junction. Skull Base Surg 6:83–94.
Robinson A. (ed.) 1918. Cunningham's textbook of anatomy. 5th Ed. New York: William Wood and Company.
Roth M. 1986. Cranio-cervical growth collision: Another explanation of the Arnold-Chiari malformation and of basilar impression. Neuroradiology 28:187–194.
Schady W, Metcalfe RA, Butler P. 1987. The incidence of craniocervical bony anomalies in the adult Chiari malformation. J Neurol Sci 82:193–203.
Schäfer EA, Symington J, Bryce TH. (eds.) 1908. Quain's Elements of Anatomy, Vol. 1: Embryology. 11th Ed. New York: Longmans, Green, and Co.
Scheuer L, Black SM. 2004. The Juvenile Skeleton. San Diego: Elsevier Academic Press. p 195.
Sensenig EC. 1957. The early development of the human vertebral column. Contr Embryol Carneg Inst 33:21–41.
Shah A, Goel A. 2010. Clival dysgenesis associated with Chiari Type 1 malformation and syringomyelia. J Clin Neurosci 17:400–401.
Shapiro R, Robinson F. 1976. Embryogenesis of the human occipital bone. AJR Am J Roentgenol 126:1063–1068.
Shoja MM, Loukas M, Tubbs RS.2012a. Persistence of proatlas in man (Comment on "Occipitocervical malformation with atlas duplication"). J Neurol Neurosurg Psych doi:10.1002/ca.23051 [Epub ahead of print].
Shoja MM, Johal J, Oakes WJ, Tubbs RS. 2017b. Embryology and pathophysiology of the Chiari I and II malformations: A comprehensive review. Clin Anat.
Smith JS, Shaffrey CI, Abel MF, Menezes AH. 2010. Basilar invagination. Neurosurgery 66:39–47.

Smoker WR. 1994. Craniovertebral junction: Normal anatomy, craniometry, and congenital anomalies. Radiographics 14:255–277.

Srivastava HC. 1977. Development of ossification centres in the squamous portion of the occipital bone in man. J Anat 124:643–649.

Srivastava HC. 1992. Ossification of the membranous portion of the squamous part of the occipital bone in man. J Anat 180:219–224.

Stratemeier PH, Jensen SR. 1980. Partial regressive occipital vertebra. Neuroradiology 19:47–49.

Taitz C. 2000. Bony observations of some morphological variations and anomalies of the craniovertebral region. Clin Anat 13:354–360.

Tillmann B, Lorenz R. 1978. The stress at the human atlanto-occipital joint. I. the development of the occipital condyle. Anat Embryol (Berl) 153:269–277.

Tsuang FY, Chen JY, Wang YH, Lai DM. 2011. Neurological picture. Occipitocervical malformation with atlas duplication. J Neurol Neurosurg Psychiatry 82:1101–1102.

Tubbs RS, Grabb P, Spooner A, Wilson W, Oakes WJ. 2000. The apical ligament: Anatomy and functional significance. J Neurosurg 92:197–200.

Tubbs RS, Salter EG, Oakes WJ. 2005. Duplication of the occipital condyles. Clin Anat 18:92–95.

Tubbs RS, Salter EG, Oakes WJ. 2007. Does the mendosal suture exist in the adult? Clin Anat 20:124–125.

Tubbs RS, Lancaster JR, Mortazavi MM, Shoja MM, Chern JJ, Loukas M, Cohen-Gadol AA. 2011. Morphometry of the outlet of the foramen magnum in crania with atlantooccipital fusion. J Neurosurg Spine 15:55–59.

Vasudeva N, Choudhry R. 1996. Precondylar tubercles on the basiocciput of adult human skulls. J Anat 188:207–210.

Vega A, Quintana F, Berciano J. 1990. Basichondrocranium anomalies in adult Chiari type I malformation: A morphometric study. J Neurol Sci 99:137–145.

Wilson JT. 1937. On the nature and mode of origin of the foramen of Magendie. J Anat 71:423–428.

Xu S, Pang Q, Zhang K, Zhang H. 2010. Two patients with proatlas segmentation malformation. J Clin Neurosci 17:647–648.